Nonadiabatic dynamics of superfluid spin-orbit-coupled degenerate Fermi gas

Maxim Dzero,[1,2] Ammar A. Kirmani,[1] and Emil A. Yuzbashyan[3]
[1]*Department of Physics, Kent State University, Kent, Ohio 44240, USA*
[2]*Max Planck Institute for the Physics of Complex Systems, Nöthnitzer Straße 38, 01187 Dresden, Germany*
[3]*Center for Materials Theory, Rutgers University, Piscataway, New Jersey 08854, USA*
(Received 12 August 2015; published 25 November 2015)

We study a problem of nonadiabatic superfluid dynamics of spin-orbit-coupled neutral fermions in two spatial dimensions. We focus on the two cases when the out-of-equilibrium conditions are initiated by either a sudden change of the pairing strength or the population imbalance. For the case of a zero-population imbalance and within the mean-field approximation, the nonadiabatic evolution of the pairing amplitude in a collisionless regime can be found exactly by employing the method of Lax vector construction. Our main finding is that the presence of the spin-orbit coupling significantly reduces the region in the parameter space where a steady state with periodically oscillating pairing amplitude is realized. For the collisionless dynamics initiated by a sudden disappearance of the population imbalance, we obtain an exact expression for the steady-state pairing amplitude. In the general case of quenches to a state with finite population imbalance, we show that there is a region in the steady-state phase diagram where at long times the pairing amplitude dynamics is governed by the reduced number of the equations of motion in full analogy with the exactly integrable case.

DOI: 10.1103/PhysRevA.92.053626 PACS number(s): 67.85.De, 34.90.+q, 74.40.Gh

I. INTRODUCTION

Starting with the seminal paper by Gor'kov and Rashba [1], there has been a remarkable resurgence of interest in the physical properties of spin-orbit-coupled superfluids and superconductors in the past decade [2–10]. This interest is largely motivated by the theoretical discovery of topological insulators and topological superconductors in which spin-orbit coupling often plays a crucial role by giving rise to the existence of robust conducting states at a system's boundaries on a background of a gapped single-particle spectrum in a bulk [11–18]. In addition, the recent discovery of superconductivity at the interface in the oxide-based heterostructures [19–21] where the inversion symmetry is naturally broken served as additional motivation for studying both conventional and unconventional superconductivity in spin-orbit-coupled systems [22].

Of special interest are the physical properties of topological insulators and superconductors under external influences that drive these systems far from equilibrium. In particular, the concept of Floquet topological insulators has been recently developed in the context of various systems' external periodic driving, which leads to an inversion of the bands with different parity giving rise to metallic edge states [23–25]. Furthermore, several groups have generalized the idea of Floquet topological insulators to Floquet topological s-wave superconductors [26–31]. Most recently, it has been shown that topological Floquet superfluidity can be realized in systems where the periodic driving is self-generated in the process of the collisionless dynamics [32–34].

However, certain aspects of the pairing dynamics in the collisionless regime for the spin-orbit-coupled systems have not been addressed yet. The aim of this paper is to close the remaining gaps in the studies of this problem. Specifically, using both exact integrability and numerical analysis, we investigate how the presence of the spin-orbit coupling affects the behavior of the pairing amplitude at long times. We consider the standard protocol of inducing far-from-equilibrium coherent dynamics in fermionic condensates by a fast switch of one of the system's parameters. In our model we allow for a nonzero out-of-plane Zeeman field h_Z that gives rise to the population imbalance between the fermionic atoms in two hyperfine states. Here we discuss two cases: changes in the detuning frequency of the Feshbach resonance and in the population imbalance.

There are three relevant time scales in the problem: The first time is the perturbation time scale $\tau_{\rm quench}$, which we take to be instantaneous; the second time scale is governed by the dynamics of the Cooper pairs τ_Δ; and the third time scale τ_ε accounts for the relaxation due to two-particle collisions. In what follows we consider the limit $\tau_\varepsilon \to \infty$ and analyze the dynamics of the pairing amplitude at long times $t \gg \tau_\Delta$. Importantly, we also neglect the possibility for the pairing amplitude to become spatially inhomogeneous, which is equivalent to an assumption of having a system with a size much smaller than the superfluid coherence length.

Within the mean-field theory for the reduced BCS model in the weak-coupling limit, three types of steady states have been found for the quenches of the pairing strength and provided the system is initially in its ground state [35–39]: regime I, a gapless steady state with zero pairing amplitude $\Delta(t \to \infty) = 0$; regime II, a steady state with the constant pairing amplitude $\Delta(t \to \infty) = \Delta_\infty$; and regime III, a steady state described by the undamped periodic oscillations of the pairing amplitude. Interestingly, there are no qualitative changes in the steady-state phase diagram for the quenches across the s-wave Feshbach resonance [40] as well as for the two-dimensional chiral superfluids [32,33]. In principle, other steady states, such as the one in which the pairing amplitude is a multiperiod function of time, can also be realized [37,41]. However, realization of these states requires that the system is initially in an excited state.

Perhaps the most surprising result from the earlier studies of the nonadiabatic pairing problem is the discovery of a steady state with the periodically oscillating amplitude whose

analytical expression is given by the Jacobi elliptic function [35,37,41,42]. Thus, the main thrust of the present work is, on the one hand, to investigate the fate of that steady state for a condensate with equal populations and nonzero spin-orbit coupling. On the other hand, we will also investigate whether in the model with the population imbalance a system allows the realization of that steady state, i.e., the pairing amplitude is still expressed in terms of the Jacobi elliptic function, even though nonzero-population imbalance precludes the full analytical description.

Let us briefly summarize our results. In the first part of the paper we analyze the effect of the spin-orbit coupling on the steady-state phase diagram. We find that steady state III is realized in a much narrower region of the phase diagram. In particular, we find that the size of region III is inversely proportional to the strength of the spin-orbit coupling. Qualitatively, this effect is due to the lifting of the Kramers degeneracy by the spin-orbit coupling. Since the total pairing amplitude is determined by the pairing in two chiral bands and the collective collisionless dynamics is reduced to a motion of two effective variables, large spin-orbit coupling effectively hinders the appearance of the steady state with periodically oscillating amplitude.

The remaining part of our discussion concerns the nature of the steady state for the quenches in the population imbalance. This problem has been recently studied by Dong *et al.* [34] by solving the Bogoliubov–de Gennes equations numerically. Here we show that for the quenches to the state with equal atomic populations, the superfluid dynamics for the pairing amplitude can in fact be found exactly. Specifically, we obtain an exact expression for the steady-state pairing amplitude and analyze the steady-state phase diagram as a function of the population imbalance in the initial state. Our results for this part are generally in agreement with those reported in Ref. [34]. Then we continue with the discussion for the quenches to a state with a finite population imbalance. For this part we have to resort to a numerical analysis of the equations of motion. Our main finding is that when the finite value of the population imbalance exceeds some critical value, we observe the dynamical reduction in the number of quantities describing the system's dynamics. In other words, the order parameter dynamics is described by the same equations of motion as in integrable case of a zero-population imbalance. This implies that we are able to find an analytical form for the pairing amplitude at long times, although the parameters of the solution cannot be determined exactly from the initial conditions.

In the next section we introduce the model, briefly review its ground-state properties, and derive the equation of motion that describes the superfluid dynamics in terms of real functions. In Sec. III we analyze the possible steady states that appear as a result of quench in the pairing strength for equal atomic populations. In the first part of Sec. IV we discuss the steady-state diagram for the quenches to the state with a zero-population imbalance, while in the second part we present the results of the numerical simulations for the quenches into a state with a nonzero-population imbalance. Section V is followed by the concluding discussion of our results. In Appendixes A and B we provide the details of the derivation of the equations of motion.

II. MODEL

Our starting point is the BCS Hamiltonian in the presence of the spin-orbit interaction in two spatial dimensions and the Zeeman magnetic field term [1,15,16,34]

$$H = \sum_{\mathbf{k}\alpha\beta} \left[\left(\xi_{\mathbf{k}} \delta_{\alpha\beta} - h_Z \sigma^z_{\alpha\beta} \right) + \alpha_{\mathrm{SO}} (\vec{\Gamma}_{\mathbf{k}} \cdot \vec{\sigma}) \right] \hat{c}^\dagger_{\mathbf{k}\alpha} \hat{c}_{\mathbf{k}\beta} - g \sum_{\mathbf{k}\mathbf{k}'} \hat{c}^\dagger_{\mathbf{k}\uparrow} \hat{c}^\dagger_{-\mathbf{k}\downarrow} \hat{c}_{-\mathbf{k}'\downarrow} c_{\mathbf{k}'\uparrow}, \tag{2.1}$$

where $\hat{c}^\dagger_{\mathbf{k}\alpha}$ is a fermionic creation operator with momentum $\mathbf{k}$ and spin projection α, $g > 0$ is the pairing strength, $\vec{\Gamma}_{\mathbf{k}} = (k_y, -k_x)$, α_{SO} is the Rashba spin-orbit coupling constant, h_Z is a Zeeman field that determines the degree of the population imbalance, $\xi_{\mathbf{k}} = k^2/2 - \mu$ is the single-particle energy taken relative to the chemical potential μ, and we set the mass of the fermions to $m = 1$. In passing we note that this model, strictly speaking, is not applicable to the system of charged fermions since the orbital effects will dominate the Pauli limiting effects.

The noninteracting part of the Hamiltonian (2.1) can be diagonalized, which yields a new spectrum

$$\varepsilon_{\mathbf{k}\lambda} = \xi_{\mathbf{k}} - \lambda \sqrt{h_Z^2 + (\alpha_{\mathrm{SO}} k)^2}, \quad \lambda = \pm 1. \tag{2.2}$$

We can now perform the unitary transformation from the original operators to new operators, which describe the fermionic excitations in chiral bands. The analysis of the ground-state properties of the model (2.1) can be considerably simplified after we employ the mean-field theory approximation in the particle-particle channel and then make a unitary transformation from the original operators $\hat{c}_{\mathbf{k}\lambda}$ to a fermionic operators in chiral basis $\hat{a}_{\mathbf{k}\lambda}$. The resulting mean-field Hamiltonian reads

$$\mathcal{H} = \sum_{\mathbf{k}\lambda} \varepsilon_{\mathbf{k}\lambda} \hat{a}^\dagger_{\mathbf{k}\lambda} \hat{a}_{\mathbf{k}\lambda} - \frac{\Delta}{2} \sum_{\mathbf{k}\lambda} \lambda \eta^*_{\mathbf{k}} \Theta_k \hat{a}^\dagger_{\mathbf{k}\lambda} \hat{a}^\dagger_{-\mathbf{k}\lambda} - \frac{\overline{\Delta}}{2} \sum_{\mathbf{k}\lambda} \eta_{\mathbf{k}} \widetilde{\Theta}_k \hat{a}_{-\mathbf{k}\lambda} \hat{a}_{\mathbf{k}\bar{\lambda}} + \mathrm{H.c.} \tag{2.3}$$

Here, for convenience, we introduced the following momentum-dependent functions: $\eta_{\mathbf{k}} = \exp[i \tan^{-1}(k_y/k_x)]$ and

$$\Theta_k = \frac{\alpha_{SO} k}{R_{\mathbf{k}}}, \quad \widetilde{\Theta}_k = \frac{h_Z}{R_{\mathbf{k}}}, \quad R_{\mathbf{k}} = \sqrt{h_Z^2 + (\alpha_{\mathrm{SO}} k)^2}. \tag{2.4}$$

Formally, the model (2.3) is analogous to the model discussed by Sato *et al.* [15,16]. The crucial difference in our case, however, is that the pairing gap Δ is not proximity induced and instead must be determined self-consistently:

$$\Delta = g \sum_{\mathbf{k}\lambda} \eta_{\mathbf{k}} [\lambda \Theta_k \langle \hat{a}_{-\mathbf{k}\lambda} \hat{a}_{\mathbf{k}\lambda} \rangle + \widetilde{\Theta}_k \langle \hat{a}_{-\mathbf{k}\lambda} \hat{a}_{\mathbf{k}\bar{\lambda}} \rangle]. \tag{2.5}$$

The mean-field Hamiltonian (2.3) can be diagonalized. We find that the single-particle spectrum consists of four bands $\omega_\pm(\mathbf{k}, \lambda) = \pm E_{\mathbf{k}\lambda}$ with the dispersion

$$E_{\mathbf{k}\lambda} = \left[\xi_{\mathbf{k}}^2 + R_{\mathbf{k}}^2 + \Delta^2 - 2\lambda R_{\mathbf{k}} \sqrt{\xi_{\mathbf{k}}^2 + \widetilde{\Theta}_k^2 \Delta^2} \right]^{1/2}. \tag{2.6}$$

Before we discuss the ground-state properties of the model (2.3), we first introduce the auxiliary functions, which are analogous to the pseudospin variables for the BCS model.

A. Equations of motion

In this section we list the equations of motion (EOMs) that will allow us to study the dynamics of the pairing amplitude in the collisionless regime. Equations of motion can be obtained from the corresponding EOMs for the single-particle propagators, which can then be cast into the form of the EOMs analogous to the Bloch equations for the magnetic moments in an external magnetic field. As a reader may have already guessed, there should be ten equations of motion overall: Six equations describe the Cooper pair dynamics on each of the two chiral bands $\lambda = \pm$ and the remaining four appear as a result of a nonzero Zeeman field. The details of the derivation of the equations of motion are given in Appendix A, so here we provide the final results. The first six equations are compactly written as

$$\partial_t \vec{S}_{\mathbf{k}\lambda} = \vec{B}_{\mathbf{k}\lambda}(t) \times \vec{S}_{\mathbf{k}\lambda}(t) + \vec{m}_{\mathbf{k}}(t) \times \vec{L}_{\mathbf{k}\lambda}(t), \tag{2.7}$$

where $\vec{B}_{\mathbf{k}\lambda} = 2(-\Theta_k \Delta_x, -\Theta_k \Delta_y, \varepsilon_{\mathbf{k}\lambda})$ is an effective field around which $\vec{S}$ is precessing and the vector $\vec{m}_k = 2(-\widetilde{\Theta}_k \Delta_x, -\widetilde{\Theta}_k \Delta_y, 0)$ can be interpreted as an induced magnetization since its xy components vanish for $h_Z = 0$. Naturally, Eq. (2.7) has the form of the Bloch equations for the BCS superconductor when $h_Z = 0$. The first two components of $\vec{B}_{\mathbf{k}\lambda}$ are determined self-consistently by

$$\Delta_x(t) - i\Delta_y(t) = g \sum_{\mathbf{k}\mu} [\Theta_k S^-_{\mathbf{k}\mu}(t) + \widetilde{\Theta}_k L^-_{\mathbf{k}\mu}(t)], \tag{2.8}$$

where we have adopted the usual notation $S^{\pm} = S^x \pm i S^y$. The equations of motion for the components of vector $\vec{L}_{\mathbf{k}\lambda}(t)$ are

$$\begin{aligned}
\partial_t L^x_{\mathbf{k}\lambda} &= -2\epsilon_{\mathbf{k}} L^y_{\mathbf{k}\lambda} - \widetilde{\Theta}_k \Delta_y(t)\big[S^z_{\mathbf{k}\lambda} + S^z_{\mathbf{k}\bar{\lambda}}\big] - 2\Theta_k \Delta_x(t) T_{\mathbf{k}}, \\
\partial_t L^y_{\mathbf{k}\lambda} &= 2\epsilon_{\mathbf{k}} L^x_{\mathbf{k}\lambda} + \widetilde{\Theta}_k \Delta_x(t)\big[S^z_{\mathbf{k}\lambda} + S^z_{\mathbf{k}\bar{\lambda}}\big] - 2\Theta_k \Delta_y(t) T_{\mathbf{k}}, \\
&\partial_t L^z_{\mathbf{k}\lambda} + 2\lambda R_k T_{\mathbf{k}}(t) + \widetilde{\Theta}_k \Delta_x(t)\big[S^y_{\mathbf{k}\lambda} - S^y_{\mathbf{k}\bar{\lambda}}\big] \\
&- \widetilde{\Theta}_k \Delta_y(t)\big[S^x_{\mathbf{k}\lambda} - S^y_{\mathbf{k}\bar{\lambda}}\big] = 0,
\end{aligned} \tag{2.9}$$

where $\epsilon_{\mathbf{k}} = k^2/2$. Note that, as it follows from these equations, $L^{x,y}_{\mathbf{k}\lambda} = L^{x,y}_{\mathbf{k}\bar{\lambda}}$ and also $L^z_{\mathbf{k}\lambda} = -L^z_{\mathbf{k}\bar{\lambda}}$. Finally, the last equation of motion that determines the evolution of the auxiliary variable $T_{\mathbf{k}}$ reads

$$\partial_t T_{\mathbf{k}} + \vec{B}_{\mathbf{k}\lambda}(t) \cdot \vec{L}_{\mathbf{k}\lambda}(t) - \frac{1}{2} \sum_{\lambda} \vec{m}_{\mathbf{k}}(t) \cdot \vec{S}_{\mathbf{k}\lambda}(t) = 2\epsilon_{\mathbf{k}} L^z_{\mathbf{k}\lambda}. \tag{2.10}$$

As we can immediately observe from these equations of motion, in the absence of the Zeeman field the first six equations decouple from the rest and become equivalent to the Anderson equations of motion for the pseudospins in the BCS model [43,44]. Thus, based on this observation, we conclude that the evolution of $\vec{S}_{\mathbf{k}\lambda}(t)$ can be determined exactly [45,46]. However, for the general case of a nonzero Zeeman field, one needs to resort to the numerical solution of the equations above for the dynamics initiated by a sudden change in the parameters of the model, such as pairing strength g, Zeeman field h_Z, or spin-orbit coupling α_{SO}. In what follows we specifically study the quenches of the coupling constant and Zeeman field.

B. Initial conditions

Let us write down the expressions for the auxiliary functions $\vec{S}_{\mathbf{k}\lambda}(t)$, $\vec{L}_{\mathbf{k}\lambda}(t)$, and $T_{\mathbf{k}}(t)$ at the time of a quench $t = 0$. In what follows we focus only on the case when the system is initially in its ground state. Then the initial momentum distribution for these variables directly follows from the equations of motion (2.7), (2.9), and (2.10). Without loss of generality, we assume that initially the superfluid order parameter is real $\Delta_x = \Delta$ and $\Delta_y = 0$. Employing the relations between the single-particle propagators, evaluated at equal times and auxiliary functions above, for the x components of $\vec{S}_{\mathbf{k}\lambda}(t)$ and $\vec{L}_{\mathbf{k}\lambda}(t)$ we find

$$\begin{aligned}
S^x_{\mathbf{k}\lambda}(0) &= \frac{\Theta_k \Delta\big(E_{\mathbf{k}\lambda} E_{\mathbf{k}\bar{\lambda}} + \varepsilon^2_{\mathbf{k}\bar{\lambda}} + \Delta^2\big)}{2E_{\mathbf{k}\lambda} E_{\mathbf{k}\bar{\lambda}}(E_{\mathbf{k}\lambda} + E_{\mathbf{k}\bar{\lambda}})}, \\
L^x_{\mathbf{k}\lambda}(0) &= \frac{\widetilde{\Theta}_k \Delta[E_{\mathbf{k}\lambda} E_{\mathbf{k}\bar{\lambda}} + \varepsilon_{\mathbf{k}\lambda}\varepsilon_{\mathbf{k}\bar{\lambda}} + \Delta^2]}{2E_{\mathbf{k}\lambda} E_{\mathbf{k}\bar{\lambda}}(E_{\mathbf{k}\lambda} + E_{\mathbf{k}\bar{\lambda}})},
\end{aligned} \tag{2.11}$$

while $S^y_{\mathbf{k}\lambda}(0) = L^y_{\mathbf{k}\lambda}(0) = T_{\mathbf{k}} = 0$. Reader can easily check that in the limit $h_Z = 0$ we recover the expression for the Anderson pseudospin in the BCS model. Consequently, in the limit of $\alpha_{\mathrm{SO}} = 0$ we naturally find $S^x_{\mathbf{k}\lambda}(0) = 0$, while $L^x_{\mathbf{k}\lambda}(0) = \varphi_{\mathbf{k}}\Delta/2E_{\mathbf{k}}$ with $E_{\mathbf{k}} = \sqrt{(\epsilon_{\mathbf{k}} - \mu)^2 + \Delta^2}$ and $\varphi_{\mathbf{k}} = E_{\mathbf{k}}[1 + \mathrm{sgn}(E_{\mathbf{k}} - h_Z)]/(E_{\mathbf{k}} + h_Z + |E_{\mathbf{k}} - h_Z|)$. Similarly, for $S^z_{\mathbf{k}\lambda}(0)$ and $L^z_{\mathbf{k}\lambda}(0)$ we obtain

$$\begin{aligned}
L^z_{\mathbf{k}\lambda}(0) &= \frac{\Theta_k \widetilde{\Theta}_k \Delta^2(\varepsilon_{\mathbf{k}\bar{\lambda}} - \varepsilon_{\mathbf{k}\lambda})}{2E_{\mathbf{k}\lambda} E_{\mathbf{k}\bar{\lambda}}(E_{\mathbf{k}\lambda} + E_{\mathbf{k}\bar{\lambda}})}, \\
S^z_{\mathbf{k}\lambda}(0) &= -\frac{\varepsilon_{\mathbf{k}\lambda}}{\Theta_k \Delta} S^x_{\mathbf{k}\lambda}(0) + \frac{\widetilde{\Theta}_k}{\Theta_k} L^z_{\mathbf{k}\lambda}(0).
\end{aligned} \tag{2.12}$$

One can easily check that in the limit $h_Z = 0$ we recover the usual expression for $S^z_{\mathbf{k}\lambda}(0)$ in the reduced BCS model. For the case of a finite Zeeman field and no spin-orbit coupling $L^z_{\mathbf{k}\lambda}$ is zero, while $\Delta[S^z_{\mathbf{k}\lambda}(0)]_{\alpha_{\mathrm{SO}}=0} = -(\epsilon_{\mathbf{k}} - \mu)[L^x_{\mathbf{k}\lambda}(0)]_{\alpha_{\mathrm{SO}}=0}$. In this case there is a similar decoupling in the equations of motion and we only need to solve six dynamics equations instead of ten. As it turns out, the pairing dynamics in this case can be found exactly [47]. Next we discuss the ground-state properties of our mean-field model.

C. Ground state

In the absence of spin-orbit coupling superconductivity becomes energetically unfavorable when the magnitude of the Zeeman field is $h_Z > \sqrt{2}\Delta$, which is known as the Clogston-Chandrasekar criterion [48,49]. Nonzero spin-orbit coupling, however, leads to the mixing between singlet and triplet components in the anomalous Gor'kov-Rashba correlation functions [1] and superconductivity extends to much higher values of the Zeeman field.

The value of the pairing amplitude in the ground state is determined from the solution of the self-consistency

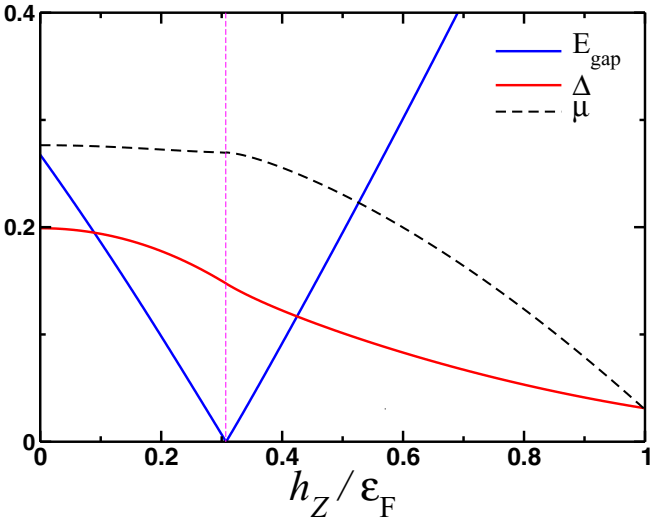

FIG. 1. (Color online) Dependence of the pairing amplitude Δ, chemical potential μ, and spectral gap $E_{\rm gap} = E_{\mathbf{k}=0,\lambda=+}$ (all in arbitrary units) as a function of the Zeeman field h_Z determined by the numerical solution of the self-consistency equations (2.13) and (2.14). Note that the superfluid becomes gapless while the order parameter remains finite at some critical value of the field $h_Z^{(c)} = \sqrt{\mu^2 + \Delta^2}$. These results correspond to the following choice of parameters: $n_c = 0.125$, $\varepsilon_F = 2\pi n_c = 0.785$, and $\alpha_{\rm SO} = 0.752$.

equation (2.8). Taking into account Eqs. (2.11) above, we find

$$\frac{1}{g} = \sum_{\mathbf{k}\lambda} \frac{E_{\mathbf{k}\lambda}E_{\mathbf{k}\bar{\lambda}} + \Delta^2 + \Theta_k^2\varepsilon_{\mathbf{k}\bar{\lambda}}^2 + \widetilde{\Theta}_k^2\varepsilon_{\mathbf{k}\lambda}\varepsilon_{\mathbf{k}\bar{\lambda}}}{2E_{\mathbf{k}\lambda}E_{\mathbf{k}\bar{\lambda}}(E_{\mathbf{k}\lambda} + E_{\mathbf{k}\bar{\lambda}})}. \tag{2.13}$$

In addition, we need to compute the value of the chemical potential μ in the ground state. The equation for the chemical potential is obtained from the standard expression for the particle number in terms of the functions $S^z_{\mathbf{k}\lambda}$. We find

$$2n_c = \sum_{\mathbf{k}\lambda}\left[\frac{1}{2} - \frac{\varepsilon_{\mathbf{k}\lambda}\left(E_{\mathbf{k}\lambda}E_{\mathbf{k}\bar{\lambda}} + \varepsilon^2_{\mathbf{k}\bar{\lambda}} + \Theta_k^2\Delta^2\right)}{2E_{\mathbf{k}\lambda}E_{\mathbf{k}\bar{\lambda}}(E_{\mathbf{k}\lambda} + E_{\mathbf{k}\bar{\lambda}})} + \frac{\widetilde{\Theta}_k^2\Delta^2\varepsilon_{\mathbf{k}\bar{\lambda}}}{2E_{\mathbf{k}\lambda}E_{\mathbf{k}\bar{\lambda}}(E_{\mathbf{k}\lambda} + E_{\mathbf{k}\bar{\lambda}})}\right], \tag{2.14}$$

where we used the relation $\Theta_k^2 + \widetilde{\Theta}_k^2 = 1$, $n_c = \varepsilon_F/2\pi$ is a particle density per spin in two dimensions, and ε_F is the Fermi energy. We analyze both of these equations numerically and present the results of our analysis in Fig. 1. Perhaps the most remarkable feature of our results is the vanishing of the spectral gap $E_{\rm gap} = E_{\mathbf{k}=0,\lambda=+}$ at some critical value of the Zeeman field $h_{Zc} = \sqrt{\mu^2 + \Delta^2}$, while the pairing amplitude remains finite. This effect is well understood: It signals a topological phase transition at which the winding number W changes from $W = 0$ to $W = 1$ (for a related discussion see, e.g., Ref. [34] and references therein). The change in the winding number reflects the appearance of the Majorana gapless chiral edge modes in a sample with boundaries.

III. QUENCH OF THE PAIRING STRENGTH IN THE MODEL WITH A ZERO-POPULATION IMBALANCE

In this section we consider the pairing dynamics following the sudden change of the pairing strength for equal atomic populations $h_Z = 0$. In this case $\Theta_k = 1$ and $\widetilde{\Theta}_k = 0$. We mainly focus of the details of the steady-state phase diagram, ignoring other aspects of the problem such as the long-time asymptote of the pairing amplitude and steady-state quasiparticle distribution function due to the similarity to the corresponding problem discussed in great detail by Yuzbashyan *et al.* [40].

A. Lax vector

Here we introduce quantities that we will later use to analyze the steady-state dynamics of the condensate. The Lax vector for our problem is defined according to

$$\vec{\mathcal{L}}(u) = \sum_{\mathbf{k}\lambda} \frac{\vec{S}_{\mathbf{k}\lambda}}{u - \varepsilon_{\mathbf{k}\lambda}} - \frac{\vec{e}_z}{g}. \tag{3.1}$$

The equation of motion for the Lax vector follows directly from the equations of motion for the pseudospins $\vec{S}_{\mathbf{k}\lambda}$:

$$\partial_t\vec{\mathcal{L}}(u) = [-2\vec{\Delta}(t) + 2u\vec{e}_z] \times \vec{\mathcal{L}}(u). \tag{3.2}$$

The square of the Lax vector is conserved by the evolution

$$\vec{\mathcal{L}}^2(u) = \frac{1}{g^2} + \sum_{\mathbf{p}\lambda}\left[\frac{2\mathcal{H}_{\mathbf{p}\lambda}}{u - \varepsilon_{\mathbf{p}\lambda}} + \frac{\vec{S}^2_{\mathbf{p}\lambda}}{(u - \varepsilon_{\mathbf{p}\lambda})^2}\right], \tag{3.3}$$

where we have introduced

$$\mathcal{H}_{\mathbf{p}\lambda} = \sum_{\mathbf{p}\lambda\neq\mathbf{q}\mu} \frac{\vec{S}_{\mathbf{p}\lambda}\cdot\vec{S}_{\mathbf{q}\mu}}{\varepsilon_{\mathbf{p}\lambda} - \varepsilon_{\mathbf{q}\mu}} - \frac{S^z_{\mathbf{p}\lambda}}{g}. \tag{3.4}$$

Following the arguments of Ref. [40], we immediately conclude that the dynamics governed by the mean-field Hamiltonian (2.1) with $h_Z = 0$ can be determined exactly.

Our main goal in this section is to determine the steady-state phase diagram, which we will plot in the plane of initial and final values of the superfluid order parameters Δ_{0i} and Δ_{0f}, just like it was done in earlier works [32,34,40].

As it has been extensively discussed in Ref. [40], in the thermodynamic limit the imaginary part of the complex roots of the spectral polynomial determines the value of the pairing amplitude in a steady state. Let us compute the roots of (3.3) for the initial configuration of the pseudospins. It follows that

$$\mathcal{L}_x(u, g_i) = \sum_{\mathbf{k}\lambda} \frac{S^x_{\mathbf{k}\lambda}}{u - \varepsilon_{\mathbf{k}\lambda}} = \Delta_{0i}\mathcal{L}_0(u), \tag{3.5}$$

where

$$\mathcal{L}_0(u) = \sum_{\mathbf{k}\lambda} \frac{1}{2(u - \varepsilon_{\mathbf{k}\lambda})\sqrt{(\varepsilon_{\mathbf{k}\lambda} - \mu)^2 + \Delta_{0i}^2}}. \tag{3.6}$$

Similarly, $\mathcal{L}_y(u, g_i) = 0$ and

$$\mathcal{L}_z(u, g_i) = -(u - \mu)\mathcal{L}_0(u). \tag{3.7}$$

Thus, Eq. (3.3) becomes

$$\left[(u - \mu)^2 + \Delta_{0i}^2\right]\mathcal{L}_0^2(u) = 0. \tag{3.8}$$

Clearly, Eq. (3.8) has the complex-conjugate pair of roots

$$u_{0,\pm} = \mu \pm i\Delta_{0i} \tag{3.9}$$

and the imaginary part of $u_{0,\pm}$ gives the value of the pairing amplitude We also define a spectral polynomial

$$Q_{2N+2}(u) = g^2 \prod_{\mathbf{p}\lambda} (u - \varepsilon_{\mathbf{p}\lambda})^2 \cdot \mathcal{L}^2(u), \tag{3.10}$$

where N is the total number of distinct single-particle energy levels $\varepsilon_{\mathbf{p}\lambda}$. Since we are considering the case when the pairing strength changes abruptly from $g_i \to g_f$, we set $g = g_f$ in Eqs. (3.1) and (3.10).

B. Roots of the spectral polynomial and steady-state diagram

For the case when the coupling is changed instantaneously, the complex roots of Eq. (3.3) or, equivalently, the roots of the spectral polynomial (3.10) with $g = g_f$ can be obtained from

$$\frac{\tilde{\beta}}{u - \mu \mp i\Delta_{0i}} + \sum_{\mathbf{k}\lambda} \frac{1}{2(u - \varepsilon_{\mathbf{k}\lambda})\sqrt{(\varepsilon_{\mathbf{k}\lambda} - \mu)^2 + \Delta_{0i}^2}} = 0, \tag{3.11}$$

where $\tilde{\beta} = g_f^{-1} - g_i^{-1}$. To analyze Eq. (3.11) it is convenient to go from summations over momentum to the integration over energy by introducing the density of states $\nu(\epsilon) = \nu_F$, where $\nu_F = n_c/\varepsilon_F$ with ε_F the Fermi energy and n_c the particle density per spin. We need to consider the contribution from each chiral band separately.

Consider $\lambda = +$ first with $\varepsilon_{\mathbf{k}+} = k^2/2 - \alpha_{\mathrm{SO}} k$:

$$\sum_{\mathbf{k}} F(\varepsilon_{\mathbf{k}+}) = \int_0^{\alpha} \frac{kdk}{2\pi} F(\varepsilon_{\mathbf{k}+}) + \int_{\alpha}^{\infty} \frac{kdk}{2\pi} F(\varepsilon_{\mathbf{k}+}). \tag{3.12}$$

Next we introduce an integration variable $\epsilon = k^2/2 - \alpha_{\mathrm{SO}} k$, giving

$$k_{\pm}(\epsilon) = \alpha_{\mathrm{SO}} \left(1 \pm \sqrt{1 + \frac{2\epsilon}{\alpha_{\mathrm{SO}}^2}} \right). \tag{3.13}$$

For the first integral in (3.12) we need to pick $k_-(\epsilon)$ while in the second integral we pick $k_+(\epsilon)$. It follows that

$$\sum_{\mathbf{k}} F(\varepsilon_{\mathbf{k}+}) = \int_{-\alpha_{\mathrm{SO}}^2/2}^{0} \frac{d\epsilon}{2\pi} \frac{2\alpha_{\mathrm{SO}}}{\sqrt{\alpha_{\mathrm{SO}}^2 + 2\epsilon}} F(\epsilon) + \int_0^{\infty} \frac{d\epsilon}{2\pi} \left(1 + \frac{\alpha_{\mathrm{SO}}}{\sqrt{\alpha_{\mathrm{SO}}^2 + 2\epsilon}} \right) F(\epsilon). \tag{3.14}$$

The contribution from the chiral band $\lambda = -$ is trivial and yields

$$\sum_{\mathbf{k}} F(\varepsilon_{\mathbf{k}-}) = \int_0^{\infty} \frac{d\epsilon}{2\pi} \left(1 - \frac{\alpha_{\mathrm{SO}}}{\sqrt{\alpha_{\mathrm{SO}}^2 + 2\epsilon}} \right) F(\epsilon). \tag{3.15}$$

Thus, Eq. (3.11) becomes

$$\frac{\beta}{u - \mu \mp i\Delta_{0i}} + \int_0^{\omega_D} \frac{d\epsilon}{2(u - \epsilon)\sqrt{(\epsilon - \mu)^2 + \Delta_{0i}^2}} + \int_{-\alpha_{\mathrm{SO}}^2/2}^{0} \frac{\alpha_{\mathrm{SO}} d\epsilon}{2\sqrt{\alpha_{\mathrm{SO}}^2 + 2\epsilon}(u - \epsilon)\sqrt{(\epsilon - \mu)^2 + \Delta_{0i}^2}} = 0, \tag{3.16}$$

where $\beta = \tilde{\beta}/2\nu_F$ and ω_D is the bandwidth. Naturally, when $\alpha_{\mathrm{SO}} = 0$ we recover the equation for the Lax roots in the BCS model. Although in the subsequent analysis we can safely take $\omega_D \to \infty$, in numerical calculations we have to keep the bandwidth finite.

We are interested in finding the values of β for which Eq. (3.16) will have two pairs of complex-conjugate roots. Let us introduce the following variable:

$$u = \mu + v\Delta_{0i}. \tag{3.17}$$

The imaginary roots that determine the value of the pairing amplitude in the steady state are determined by setting

$$u \to u \pm i\delta. \tag{3.18}$$

Using (3.17) we rewrite (3.16) as follows:

$$\frac{2\beta(v \pm i)}{v^2 + 1} + \int_{-\mu/\Delta_{0i}}^{\infty} \frac{d\epsilon}{(v - \epsilon)\sqrt{\epsilon^2 + 1}} + \sqrt{\frac{\alpha_{\mathrm{SO}}^2}{2\Delta_{0i}}} \int_{-(\alpha_{\mathrm{SO}}^2 + 2\mu)/2\Delta_{0i}}^{-\mu/\Delta_i} \times \frac{d\epsilon}{\sqrt{\epsilon + \left[(\alpha_{\mathrm{SO}}^2 + 2\mu)/2\Delta_{0i}\right]}(v - \epsilon)\sqrt{\epsilon^2 + 1}} = 0. \tag{3.19}$$

Let us find the critical value of β when the imaginary part of v becomes nonzero for the first time. We have

$$\pm\frac{2\beta}{v^2 + 1} \mp \frac{\pi\vartheta(v\Delta_{0i} + \mu)}{\sqrt{v^2 + 1}} \mp \sqrt{\frac{\alpha_{\mathrm{SO}}^2}{2\Delta_{0i}}} \frac{\pi\vartheta(-v\Delta_{0i} - \mu)\vartheta\left(2v\Delta_i + 2\mu + \alpha_{\mathrm{SO}}^2\right)}{\sqrt{v + \left[(\alpha_{\mathrm{SO}}^2 + 2\mu)/2\Delta_{0i}\right]}\sqrt{v^2 + 1}} = 0,$$

$$\frac{2\beta v}{v^2 + 1} + \int_{-\mu/\Delta_{0i}}^{\infty} \frac{d\epsilon}{(v - \epsilon)\sqrt{\epsilon^2 + 1}} + \sqrt{\frac{\alpha_{\mathrm{SO}}^2}{2\Delta_{0i}}} \int_{-(\alpha_{\mathrm{SO}}^2 + 2\mu)/2\Delta_{0i}}^{-\mu/\Delta_{0i}} \frac{d\epsilon}{\mathcal{R}(\epsilon)} = 0, \tag{3.20}$$

where we introduced for brevity the function

$$\mathcal{R}(\epsilon) = \sqrt{\epsilon + \frac{\alpha_{\mathrm{SO}}^2 + 2\mu}{2\Delta_{0i}}}(v - \epsilon)\sqrt{\epsilon^2 + 1}.$$

Let us analyze the first of Eqs. (3.20). Depending on the value of v, there are two possible solutions. The first solution corresponds to the usual BCS case

$$|\beta_c| = \frac{\pi}{2}\sqrt{v^2 + 1}, \quad v > -\mu/\Delta_{0i}, \tag{3.21}$$

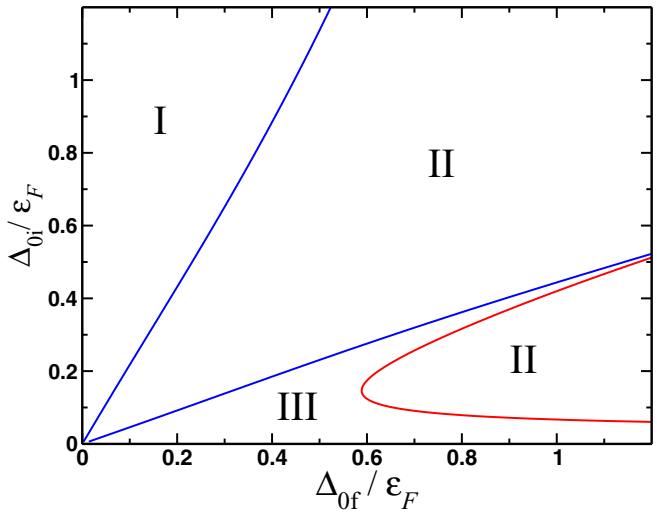

FIG. 2. (Color online) Steady-state diagram for the case $h_Z = 0$. In region I $\Delta(t \to \infty) = 0$. In region II $\Delta(t \to \infty) = \Delta_\infty$. In region III $\Delta(t)$ varies periodically with time. The parameters are $n_c = 0.125$ and $\alpha_{\rm SO} = 0.75$. In the limit of zero spin-orbit coupling the red line inside region III is absent.

while v is found by solving

$$\frac{\pi\,\mathrm{sgn}(\beta_c)}{\sqrt{v^2+1}} + \int_{-\mu/\Delta_{0i}}^{\infty} \frac{d\epsilon}{(v-\epsilon)\sqrt{\epsilon^2+1}} + \sqrt{\frac{\alpha_{\rm SO}^2}{2\Delta_{0i}}} \int_{-(\alpha_{\rm SO}^2+2\mu)/2\Delta_{0i}}^{-\mu/\Delta_{0i}} \frac{d\epsilon}{\mathcal{R}(\epsilon)} = 0 \qquad (3.22)$$

still for $v \geqslant -\mu/\Delta_{0i}$. There is, however, another solution for β_c given by

$$|\beta_c| = \frac{\pi\alpha_{\rm SO}}{2} \frac{\sqrt{v^2+1}}{\sqrt{2\Delta_{0i}v + \alpha_{\rm SO}^2 + 2\mu}}, \quad v \leqslant -\mu/\Delta_{0i}. \qquad (3.23)$$

The value of v in this case will be given by

$$\frac{\pi\alpha_{\rm SO}\mathrm{sgn}(\beta_c)}{\sqrt{v^2+1}\sqrt{2\Delta_{0i}v + \alpha_{\rm SO}^2 + 2\mu}} + \int_{-\mu/\Delta_{0i}}^{\infty} \frac{d\epsilon}{(v-\epsilon)\sqrt{\epsilon^2+1}} + \sqrt{\frac{\alpha_{\rm SO}^2}{2\Delta_{0i}}} \int_{-(\alpha_{\rm SO}^2+2\mu)/2\Delta_{0i}}^{-\mu/\Delta_{0i}} \frac{d\epsilon}{\mathcal{R}(\epsilon)} = 0 \qquad (3.24)$$

for $v \leqslant -\mu/\Delta_{0i}$.

The results of our analysis of equations for the critical β above are shown in Fig. 2. The presence of the spin-orbit coupling leads to the appearance of the region where the pairing amplitude goes to a constant (region II) realized inside the region where the pairing amplitude periodically varies with time (region III).

IV. QUENCH OF THE POPULATION IMBALANCE

As we have seen already, the nonzero Zeeman field breaks integrability. Thus, for the quenches of the Zeeman field $h_{Zi} \to h_{Zf}$ one needs to resort to the numerical analysis of the equations of motion. The main interest in studying this particular type of quench is mainly motivated by the existence of the topological transition. The task of analyzing a steady-state diagram for an arbitrary value of h_{Zf} has been recently accomplished by Dong *et al.* [34] However, as it became clear from our discussion above, for the spatial quenches such that $h_{Zf} = 0$ the problem can be analyzed analytically using the same method of Lax vector construction. The only difference from the previous analysis is that an initial pseudospin distribution explicitly depends on h_{Zi}.

A. Integrable dynamics: $h_{Zf} = 0$

We start with the analysis of the expression for the Lax vector (3.1). The expression for $\mathcal{L}_z(u)$ can be considerably simplified if we take into account the self-consistency equation (2.13). However, one needs to be careful, since at large fields the self-consistency equation does not have a solution and we have to set $\Delta = \Delta_{0i} = 0$ in (3.1). Therefore, we have to consider two cases: In the first case Δ_{0i} in the initial state is nonzero, while in the second case h_Z is large enough so that $\Delta_{0i} = 0$.

We first analyze the roots for the case of finite Δ_{0i}. The roots are the computed numerically from

$$\sum_{\mathbf{k}\lambda} \frac{(u-\mu+i\Theta_k\Delta)\left(E_{\mathbf{k}\lambda}E_{\mathbf{k}\bar{\lambda}} + \Delta^2 + \varepsilon_{\mathbf{k}\bar{\lambda}}^2\right)}{2(u-\mu-\varepsilon_{\mathbf{k}\lambda})E_{\mathbf{k}\lambda}E_{\mathbf{k}\bar{\lambda}}(E_{\mathbf{k}\lambda}+E_{\mathbf{k}\bar{\lambda}})} + \sum_{\mathbf{k}\lambda} \frac{\widetilde{\Theta}_k^2\Delta^2(\varepsilon_{\mathbf{k}\bar{\lambda}} - \varepsilon_{\mathbf{k}\lambda})}{2(u-\mu-\varepsilon_{\mathbf{k}\lambda})E_{\mathbf{k}\lambda}E_{\mathbf{k}\bar{\lambda}}(E_{\mathbf{k}\lambda}+E_{\mathbf{k}\bar{\lambda}})} = \sum_{\mathbf{k}\lambda} \frac{h_Z^2}{E_{\mathbf{k}\lambda}E_{\mathbf{k}\bar{\lambda}}(E_{\mathbf{k}\lambda}+E_{\mathbf{k}\bar{\lambda}})}, \qquad (4.1)$$

which follows from (3.1) and the self-consistency equation (2.13). We analyze this equation numerically and plot the results in Fig. 3. As expected, for relatively small values of $h_{Zi} = h_Z$ there is only one complex root, which means that the steady-state order parameter asymptotically approaches a constant. As the value of the field is increased further, it reaches h_{c2} where the second complex-conjugate root appears. For quenches of the Zeeman field with $h_Z > h_{c2}$ the pairing amplitude periodically oscillates in time. Our results confirm those found from the numerical simulations [34]. Indeed, in Fig. 4 we show $\Delta(t)$ found by numerically solving the equations of motions for various values of h_Z; it is clearly in agreement with our analysis of the Lax roots, Fig. 3.

In Fig. 5 we also plot the dependence of h_{c2} on $\alpha_{\rm SO}$, which we determine by setting $u = u_0 + i\delta$ in (IV A) and solving them together with Eqs. (2.13) and (2.14). As one may have expected, $h_{c2} \propto \alpha_{\rm SO} p_F$. Furthermore, the fact that we do not find a solution for small $\alpha_{\rm SO}$ is in qualitative agreement with the observation that the steady state with an oscillating pairing amplitude generally appears for moderate to strong quenches.

Next we would like to show that no more complex roots appear at large fields when Δ_{0i} is infinitesimally small. First, let us consider the case when the self-consistency equation (2.13) does not have a solution and, as before, we set $u = u_0 + i\delta$. Then, in the equation for the Lax roots $\mathcal{L}_z(u) = \pm i\mathcal{L}_x(u)$ we can consider the real and imaginary parts separately. The equation for the imaginary part is satisfied

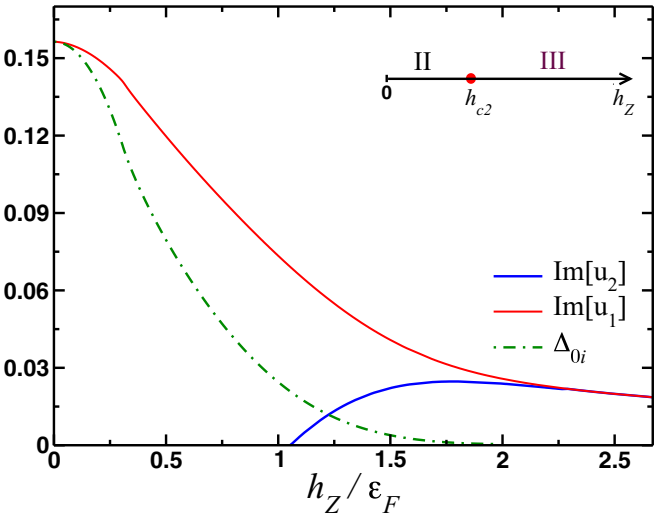

FIG. 3. (Color online) Imaginary parts of the roots of $\mathcal{L}^2(u) = 0$ and superfluid order parameter Δ_{0i} in the initial state plotted as a function of the initial value of the Zeeman field $h_{Zi} = h_Z$ for the quenches $h_{Zi} \to h_{Zf} = 0$. Note that the imaginary parts of both roots essentially coincide with each other for the initial conditions with $\Delta_{0i} \to 0$. At $h_Z = h_{c2}$ the second complex root appears. Thus, h_{c2} separates the steady states with constant and periodically oscillating superfluid order parameters. These results correspond to the following choice of parameters: $n_c = 0.125$, $\varepsilon_F = 0.785$, and $\alpha_{SO} = 0.752$.

only if $u_0 < -h_Z$, while the equation of the real part reads

$$\frac{2}{g} + \sum_{\mathbf{k}\lambda} P\left(\frac{\mathrm{sgn}(\varepsilon_{\mathbf{k}\lambda})}{u_0 - \mu - \varepsilon_{\mathbf{k}\lambda}}\right) = 0, \tag{4.2}$$

where P stands for the principal value. We have analyzed this equation and did not find a value of coupling g consistent with the zero value of the superfluid gap. We reach the same conclusion from the analysis of Eq. (4.1) for the case when Δ_{0i} is small enough, so it can be neglected. To summarize, we find that for the quenches of the Zeeman field from some finite value h_{Zi} to zero, there are only two steady states possible at long times: In the first one $\Delta(t)$ asymptotically approaches a constant, while in the second one $\Delta(t)$ continues to oscillate periodically.

B. Analytical solution for the pairing amplitude

In this section we derive the analytic expressions for the pairing amplitude $\Delta(t)$ in a steady state. Our discussion here follows closely the related discussion in Refs. [32,40].

Steady states with constant and periodically oscillating pairing amplitudes can be described analytically by constructing the Lax vector for an effective m-pseudospin system. The Lax reduction procedure states that at long times the dynamics of a superfluid is governed by the dynamics of only a few generalized pseudospin variables, which we will denote by $\vec{\sigma}_j$ [32,40]. The Lax vector describing the reduced solution is

$$\vec{\mathcal{L}}_{\mathrm{red}}(u) = \left(1 + \sum_{\mathbf{p}\lambda} \frac{d_{\mathbf{p}\lambda}}{u - \varepsilon_{\mathbf{p}\lambda}}\right) \vec{\mathcal{L}}_m(u), \tag{4.3}$$

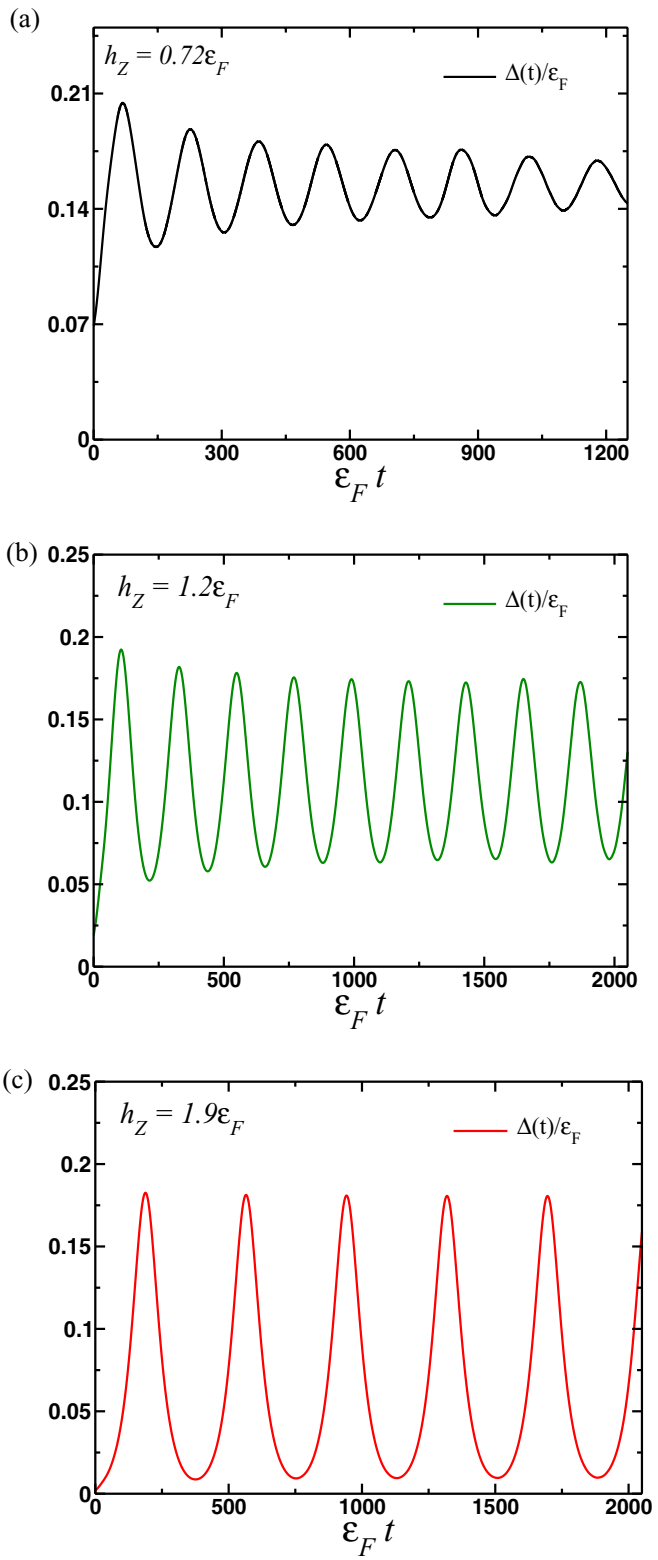

FIG. 4. (Color online) Results of the numerical solution of the equations of motion for $\Delta(t)$ in the exactly integrable case when $h_{Zf} = 0$. These results correspond to the following choice of parameters: $n_c = 0.125$, $\varepsilon_F = 0.785$, and $h_{c2} = 1.02\varepsilon_F$.

$$\vec{\mathcal{L}}_m(u) = \left(\sum_{j=1}^{m} \frac{\vec{\sigma}_j}{u - \epsilon_j} - \frac{\vec{e}_z}{g}\right).$$

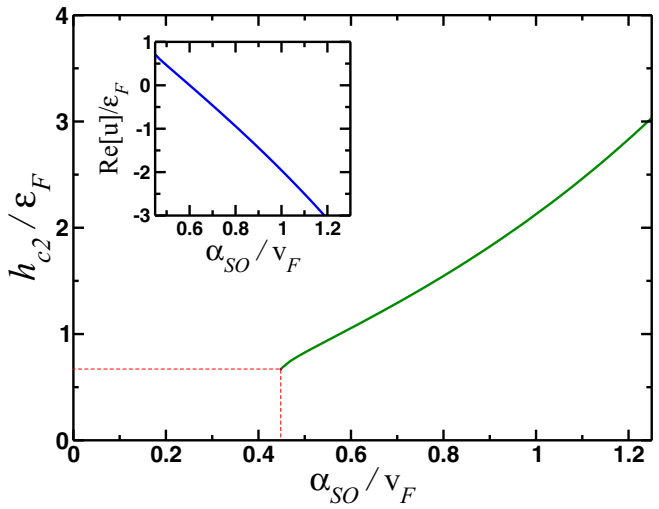

FIG. 5. (Color online) Dependence of the critical Zeeman field h_{c2}, which separates the steady states with constant and periodically oscillating pairing amplitudes, on the strength of the spin-orbit coupling. Note that for the case of weak spin-orbit coupling, the pairing amplitude will always go to a constant at long times $\Delta(t \to \infty) = \Delta_\infty$. The inset shows the dependence of the real part of the second root on α_{SO}. These results correspond to the following choice of parameters: $n_c = 0.125$ and $\varepsilon_F = 0.785$.

Here $\vec{\mathcal{L}}_m(u)$ is a Lax vector for a reduced system; the time-dependent vectors $\vec{\sigma}_j$ and parameters $d_{\mathbf{p}\lambda}$ and ϵ_j need to be determined. As it can be easily seen, vectors $\vec{\sigma}_j$ satisfy the same equations of motion as the original pseudospins $\vec{S}_{\mathbf{p}\lambda}$. The parameters of the reduced Lax vector are chosen such that

$$\vec{\mathcal{L}}(u) = \vec{\mathcal{L}}_{\rm red}(u). \tag{4.4}$$

Therefore, the equation of motion for vector $\vec{\mathcal{L}}_{\rm red}(u)$ is the same as the one for $\vec{\mathcal{L}}(u)$:

$$\partial_t \vec{\mathcal{L}}_{\rm red}(u) = [-2\vec{\Delta}(t) + 2u\vec{e}_z] \times \vec{\mathcal{L}}_{\rm red}(u), \tag{4.5}$$

where we use $\vec{\Delta} = (\Delta_x, \Delta_y)$ for brevity. By matching the residues at $u = \varepsilon_{\mathbf{p}\lambda}$ and at $u = \epsilon_j$ we find the following set of relations:

$$\sum_{\mathbf{p}\lambda} \frac{d_{\mathbf{p}\lambda}}{\epsilon_j - \varepsilon_{\mathbf{p}\lambda}} = -1, \quad j = 1, \ldots, m,$$

$$d_{\mathbf{p}\lambda} \vec{\mathcal{L}}_m(\varepsilon_{\mathbf{p}\lambda}) = \vec{S}_{\mathbf{p}\lambda}. \tag{4.6}$$

In the thermodynamic limit it is possible to find the reduced solutions that have the same integrals of motion as the solutions for the quenched dynamics, i.e., they have the same $\mathcal{L}^2(u)$. Thus, Eq. (4.3) becomes

$$1 + \sum_\lambda \int \frac{\nu_\lambda(\epsilon_\lambda) d_\lambda(\epsilon_\lambda) d\epsilon_\lambda}{u - \epsilon_\lambda} = -\zeta(u) \sqrt{\frac{\vec{\mathcal{L}}^2(u)}{\vec{\mathcal{L}}_m^2(u)}}, \tag{4.7}$$

where $\zeta(u) = \pm 1$, $\nu_\lambda(\epsilon)$ is the density of states for the chiral band λ, and $\vec{\mathcal{L}}^2(u)$ is determined by the initial conditions. By setting $u = \varepsilon \pm i\delta$ we can immediately determine $d_\lambda(\epsilon)$,

$$d_\lambda(\varepsilon) = \frac{i\zeta(\varepsilon)}{2\pi \nu_\lambda(\varepsilon)} \left(\frac{\sqrt{\mathcal{L}^2(\varepsilon_-)}}{\sqrt{\mathcal{L}_m^2(\varepsilon_-)}} - \frac{\sqrt{\mathcal{L}^2(\varepsilon_+)}}{\sqrt{\mathcal{L}_m^2(\varepsilon_+)}} \right), \tag{4.8}$$

with $\varepsilon_\pm = \varepsilon \pm i\delta$. In what follows we will derive the explicit expressions to determine the parameters $\vec{\sigma}_j$ and η_j $(j \geqslant 1)$, which define $\vec{\mathcal{L}}_m(u)$, in terms of the complex roots of $\mathcal{L}^2(u)$.

1. The m = 1 solution

This is the case of the one-spin solution. The expression for $\vec{\mathcal{L}}_{m=1}$ reads

$$\vec{\mathcal{L}}_{m=1}(u) = \frac{\vec{\sigma}_1}{u - \epsilon_1} - \frac{\vec{e}_z}{g}. \tag{4.9}$$

The relation between $\vec{\sigma}_1$ and Δ follows directly from the self-consistency equation (2.8) and Eq. (4.6):

$$\vec{\Delta}(t) = g\vec{\sigma}_1(t), \tag{4.10}$$

which also implies that σ_1^z remains constant. Using the equation of motion for the Lax vector (4.5) together with (4.10) we can now solve for $\Delta(t)$:

$$\Delta(t) = \Delta_\infty e^{2i\mu_\infty t - i\varphi_0}, \tag{4.11}$$

where $\mu_\infty = \epsilon_1 + g\sigma_1^z$ and φ_0 is an integration constant. The parameters $\{\Delta_\infty, \mu_\infty\}$ can be expressed in terms of the roots for the square of the reduced Lax vector. Recall that in the thermodynamic limit these roots are the same as the roots of $\vec{\mathcal{L}}^2(u) = 0$ by construction. As we have seen in the previous section, when $h_{Zi} \leqslant h_{c2}$ there is only one pair of complex-conjugate roots, which we define $u_\pm = u_{1\mathfrak{r}} \pm i u_{1\mathfrak{i}}$. Taking the square of both parts in Eq. (4.9) and regrouping the terms on the right-hand side yields

$$u_{1\mathfrak{r}} = \mu_\infty, \quad u_{1\mathfrak{i}} = \Delta_\infty. \tag{4.12}$$

Thus, in agreement with earlier results we find that the imaginary root of $\mathcal{L}^2(u) = 0$ determines the value of the pairing amplitude at long times.

2. The m = 2 solution

This is the case of the two-spin solution with the reduced Lax vector of the form

$$\vec{\mathcal{L}}_{m=2}(u) = \frac{\vec{\sigma}_1}{u - \epsilon_1} + \frac{\vec{\sigma}_2}{u - \epsilon_2} - \frac{\vec{e}_z}{g} \tag{4.13}$$

and

$$\vec{\Delta} = g \cdot (\vec{\sigma}_1 + \vec{\sigma}_2), \quad \Delta_x(t) - i\Delta_y(t) = \Omega e^{-i\Phi}, \tag{4.14}$$

where in the second expression $\Omega = |\vec{\Delta}|$ and Φ is the phase of the pairing amplitude. The dynamics of the variables $\vec{\sigma}_{1,2}$ is governed by the following two-spin Hamiltonian:

$$H_{m=2} = 2\left(\epsilon_1 \sigma_1^z + \epsilon_2 \sigma_2^z\right) - 2\vec{\Delta} \cdot \vec{\sigma}. \tag{4.15}$$

The z component of $\vec{\sigma} = \vec{\sigma}_1 + \vec{\sigma}_2$ is conserved by evolution governed by the reduced Hamiltonian (4.15), which reflects the total particle conservation. In addition, the total energy $\mathcal{E}$ must be conserved by the evolution. Given the self-consistency condition (4.14) for the reduced Hamiltonian, it follows that $\mathcal{E}$ is conserved provided the terms containing $\Delta(t)$ drop out from (4.15). In turn, this is only possible for $\sigma_{1,2}^z \propto \vec{\sigma}^2$. Therefore, we write [32,40]

$$\sigma_1^z = \frac{a_1}{g}\Omega^2 + b_1, \quad \sigma_2^z = \frac{a_2}{g}\Omega^2 + b_2, \tag{4.16}$$

where coefficients $a_{1,2}$ and $b_{1,2}$ satisfy

$$\begin{aligned} \epsilon_1 a_1 + \epsilon_2 a_2 = \tfrac{1}{2}, \quad 2(\epsilon_1 b_1 + \epsilon_2 b_2) = \mathcal{E}, \\ a_1 = -a_2, \quad b_1 + b_2 = \sigma^z. \end{aligned} \tag{4.17}$$

Importantly, by a virtue of the second of Eqs. (4.6) we obtain the following ansatz for the original variables:

$$S^z_{\mathbf{p}\lambda} = a_{\mathbf{p}\lambda}\Omega^2 + b_{\mathbf{p}\lambda}. \tag{4.18}$$

Furthermore, the equations of motion for the two remaining components of $\vec{S}_{\mathbf{p}\lambda}$ [Eq. (2.7) with $\vec{m} = 0$ and $\Theta_k = 1$] yield

$$S^-_{\mathbf{p}\lambda} e^{i\Phi} - S^+_{\mathbf{p}\lambda} e^{-i\Phi} = 2i a_{\mathbf{p}\lambda}\dot{\Omega}, \tag{4.19}$$

where we use the notation $S^{\pm}_{\mathbf{p}\lambda} = S^x_{\mathbf{p}\lambda} \pm i S^y_{\mathbf{p}\lambda}$. After a series of algebraic manipulations identical to the ones in Refs. [32,40], we find the following equation for Ω:

$$\begin{aligned} \dot{\Omega}^2 + \Omega^4 + \left(\frac{2b_{\mathbf{p}\lambda}}{a_{\mathbf{p}\lambda}} + 4\varepsilon^2_{\mathbf{p}\lambda}\right)\Omega^2 - 4A\varepsilon_{\mathbf{p}\lambda}\Omega \\ + A^2 + \frac{b^2_{\mathbf{p}\lambda} - S^2_{\mathbf{p}\lambda}}{a^2_{\mathbf{p}\lambda}} = 0, \end{aligned} \tag{4.20}$$

where A is a function of Ω given by

$$A = 2\mu_A\Omega + \frac{\kappa_A}{\Omega} \tag{4.21}$$

and μ_A and κ_A are arbitrary real constants. Since the same equation for Ω is found by considering the equations of motion for the variables $\vec{\sigma}_{1,2}$, we conclude that the coefficients in Eq. (4.20) must be independent of $\mathbf{p}$ and λ:

$$\begin{aligned} \frac{b_{\mathbf{p}\lambda}}{a_{\mathbf{p}\lambda}} + 2(\varepsilon_{\mathbf{p}\lambda} - \mu_A)^2 = 2\rho, \\ \frac{b^2_{\mathbf{p}\lambda} - S^2_{\mathbf{p}\lambda}}{a^2_{\mathbf{p}\lambda}} - 4\kappa_A(\varepsilon_{\mathbf{p}\lambda} - \mu_A) = 4\chi. \end{aligned} \tag{4.22}$$

Thus the differential equation for $\Omega(t)$ becomes

$$\dot{\Omega}^2 + \Omega^4 + 4\rho\Omega^2 + \frac{\kappa^2_A}{\Omega^2} + 4\chi = 0. \tag{4.23}$$

The solution of this equation is [40]

$$\Omega = \sqrt{\Lambda^2 + e_1}, \quad \Lambda = \Delta_+ \mathrm{dn}[\Delta_+(t - t_0), k'], \tag{4.24}$$

where dn is the Jacobi elliptic function, $k' = \Delta_-/\Delta_+$, $\Delta^2_- = e_2 - e_1$, $\Delta^2_+ = e_3 - e_1$, and the parameters $e_{1,2,3}$ are the real roots of the qubic polynomial

$$P_3(w) = w^3 + 4\rho w^2 + 4\chi w + \kappa^2_A. \tag{4.25}$$

The last step is to match the coefficients in the polynomial (4.25) with the values of the complex-conjugate roots appearing for $h_{Zi} > h_{c2}$ (Fig. 3). To do that we employ the relation (4.6). First we solve Eqs. (4.22) for $a_{\mathbf{p}\lambda}$ and $b_{\mathbf{p}\lambda}$. We find

$$\begin{aligned} a_{\mathbf{p}\lambda} = -\frac{S_{\mathbf{p}\lambda}}{2\sqrt{[(\varepsilon_{\mathbf{p}\lambda} - \mu_A)^2 - \rho]^2 - \kappa_A(\varepsilon_{\mathbf{p}\lambda} - \mu_A) - \chi}}, \\ b_{\mathbf{p}\lambda} = \frac{[(\varepsilon_{\mathbf{p}\lambda} - \mu_A)^2 - \rho]S_{\mathbf{p}\lambda}}{\sqrt{[(\varepsilon_{\mathbf{p}\lambda} - \mu_A)^2 - \rho]^2 - \kappa_A(\varepsilon_{\mathbf{p}\lambda} - \mu_A) - \chi}}. \end{aligned} \tag{4.26}$$

Similarly, the coefficients $a_{1,2}$ and $b_{1,2}$ of the reduced solution (4.16) are found using the conservation laws (4.17):

$$a_{1,2} = \pm\frac{1}{2(\epsilon_1 - \epsilon_2)}, \quad b_{1,2} = \pm\frac{\mathcal{E} - \epsilon_{2,1}\sigma^z}{\epsilon_1 - \epsilon_2}. \tag{4.27}$$

Using these expressions, let us match the prefactors in front of Ω^2 after we use Eqs. (4.16) and (4.18) together with (4.26) and (4.27) in the second of Eqs. (4.6) for the z components of $\mathcal{L}_m$ and $\vec{S}_{\mathbf{p}\lambda}$. We find

$$\frac{d_{\mathbf{p}\lambda}}{g} = \frac{(\varepsilon_{\mathbf{p}\lambda} - \epsilon_1)(\varepsilon_{\mathbf{p}\lambda} - \epsilon_2)S_{\mathbf{p}\lambda}}{\sqrt{[(\varepsilon_{\mathbf{p}\lambda} - \mu_A)^2 - \rho]^2 - \kappa_A(\varepsilon_{\mathbf{p}\lambda} - \mu_A) - \chi}}. \tag{4.28}$$

On the other hand,

$$d_{\mathbf{p}\lambda} = \frac{S_{\mathbf{p}\lambda}}{\sqrt{\mathcal{L}^2_{m=2}(\varepsilon_{\mathbf{p}\lambda})}}. \tag{4.29}$$

Introducing the spectral polynomial $Q_4(u)$ similar to (3.10):

$$Q_4(u) = g^2(u - \epsilon_1)^2(u - \epsilon_2)^2 \cdot \vec{\mathcal{L}}^2_{m=2}(u). \tag{4.30}$$

If we now compare (4) with (4.28) we immediately identify $Q_4(u)$ with

$$Q_4(u) = [(u - \mu_A)^2 - \rho]^2 - \kappa_A(u - \mu_A) - \chi. \tag{4.31}$$

Furthermore, since in the thermodynamic limit the complex roots of $Q_4(u)$ must match the complex roots of $\mathcal{L}^2(u)$, we can express all the parameters (4.31) in terms of two pairs of complex-conjugate roots $u_{1,2} = u_{1,2\mathrm{r}} + iu_{1,2\mathrm{i}}$:

$$\begin{aligned} \mu_A &= \frac{u_{1\mathrm{r}} + u_{2\mathrm{r}}}{2}, \\ \rho &= 3\mu^2_A - 2u_{1\mathrm{r}}u_{2\mathrm{r}} - \frac{u^2_{1\mathrm{r}} + u^2_{1\mathrm{i}} + u^2_{2\mathrm{r}} + u^2_{2\mathrm{i}}}{2}, \\ \kappa_A &= 2u_{1\mathrm{r}}\left(u^2_{2\mathrm{r}} + u^2_{2\mathrm{i}}\right) + 2u_{2\mathrm{r}}\left(u^2_{1\mathrm{r}} + u^2_{1\mathrm{i}}\right) + 4\mu_A\left(\rho - \mu^2_A\right), \\ \chi &= \kappa_A\mu_A + \left(\mu^2_A - \rho\right)^2 - \left(u^2_{1\mathrm{r}} + u^2_{1\mathrm{i}}\right)\left(u^2_{2\mathrm{r}} + u^2_{2\mathrm{i}}\right). \end{aligned} \tag{4.32}$$

We plot the dependence of the roots of $P_3(w)$ (4.25) in Fig. 6. Note that e_1, e_2, and e_3 are small for $h_Z \sim h_{c2}$. As noted in Ref. [40] for the quenches of the detuning frequency across the Feshbach resonance, the value of e_1 serves as a measure of the deviation from the weak-coupling limit when $|e_1| \ll 1$.

To summarize, Eqs. (4.32) together with (4.23) provide an exact description of the order parameter dynamics in a steady state determined by the two pairs of complex-conjugate roots of the spectral polynomial. In particular, the pairing amplitude is given by

$$|\Delta(t)| = \sqrt{e_1 + \Delta^2_+ \mathrm{dn}^2[\Delta_+(t - t_0), k']}, \tag{4.33}$$

where the parameters entering this expression are given above [Eq. (4.24)]. Note that parameter e_1 is close to zero only when $h_Z \sim h_{c2}$. It is somewhat surprising to find that $|\Delta(t)|$ is described by the weak-coupling solution [40]

$$|\Delta(t)| \propto \mathrm{dn}[\Delta_+(t - t_0), k'] \tag{4.34}$$

only at lower fields.

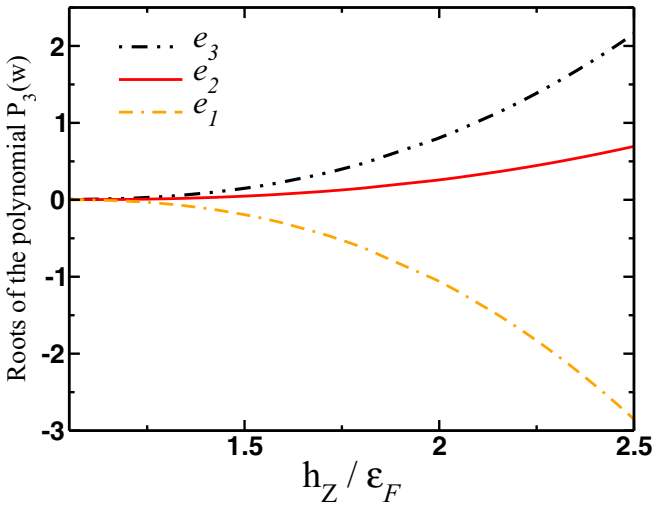

FIG. 6. (Color online) Dependence of the roots e_1, e_2, and e_3 of the qubic polynomial $P_3(w)$ [Eq. (4.25)] on the value of the imbalance h_Z. The parameters are $n_c = 0.125$ and $\varepsilon_F = 0.785$.

C. Pairing amplitude dynamics with finite population imbalance

Here we discuss the dynamics initiated by the quenches of the Zeeman field so that $h_{Zf} \neq 0$. Since the dynamics governed by the Hamiltonian (2.1) is nonintegrable, we have to resort to the numerical analysis of the equations of motion (2.7), (2.9), and (2.10). Our main motivation for this part was to check whether the steady state with the periodically oscillating pairing amplitude also extends into a nonintegrable region of the parameter space.

The time evolution of the pairing amplitude following the quench is shown in Figs. 7 and 8. We see that for certain values of h_Z/ε_F the order parameter magnitude $|\Delta(t)|$ shows oscillations with several frequencies and its amplitude is not constant at long times (at least up to the longest time scales we were able to achieve with our numerics). However, note the striking difference between the dynamics in Figs. 7 and 8: When h_{Zf} exceeds the value of $h_{c3} \approx 1.02\varepsilon_F$ provided $h_{Zi} = 1.85\varepsilon_F$, the pairing amplitude shows regular oscillations with constant amplitude. This behavior is characteristic of $\Delta(t)$, which is found in the exactly solvable limit.

To get further insight into the origin of this behavior, in Figs. 9 and 10 we plot the single-particle energy dependence of the auxiliary functions $\vec{L}(\varepsilon,t)$ and $T(\varepsilon,t)$ at long times when $h_{Zi} < h_{c3}$ and $h_{Zi} > h_{c3}$. For these plots the regular oscillatory behavior of $\Delta(t)$ becomes clear since for $h_{Zi} > h_{c3}$ the

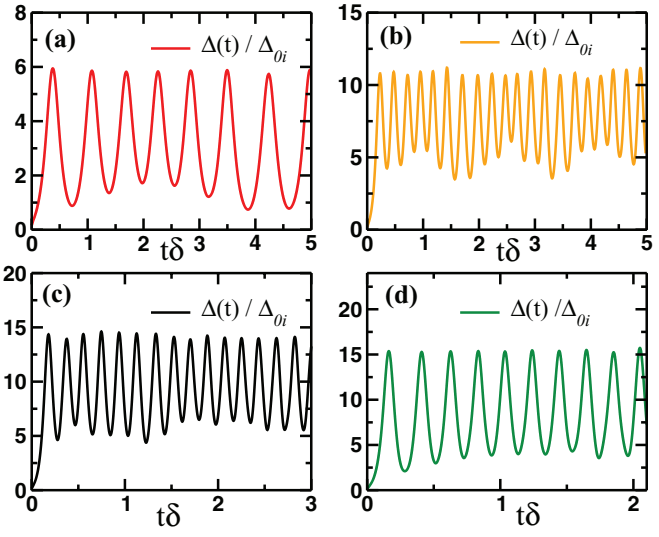

FIG. 7. (Color online) Results of the numerical solution of the equations of motion for $\Delta(t)$ in the general, i.e., nonintegrable, case $h_{Zf} \neq 0$ with (a) $h_{Zf} = 0.9\varepsilon_F$, (b) $h_{Zf} = 0.5\varepsilon_F$, (c) $h_{Zf} = 0.25\varepsilon_F$, and (d) $h_{Zf} = 0.1\varepsilon_F$. The values of the remaining parameters are $h_{Zi} = 1.85\varepsilon_F$, $n_c = 0.125$, and $\varepsilon_F = 0.785$.

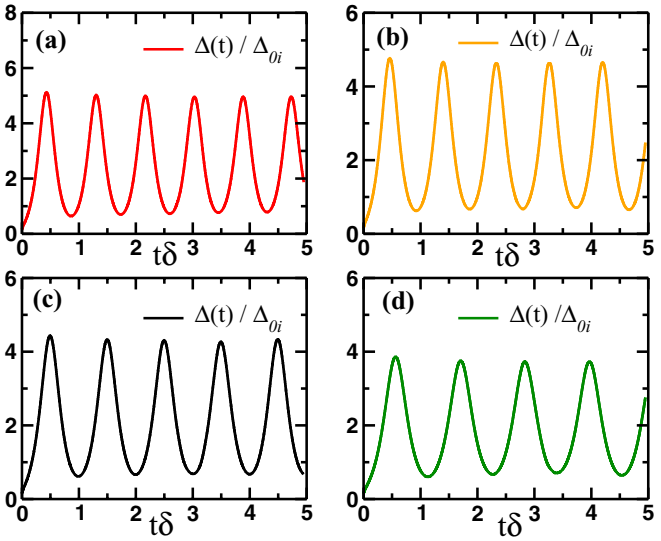

FIG. 8. (Color online) Same as Fig. 7 with (a) $h_{Zf} = 1.25\varepsilon_F$, (b) $h_{Zf} = 1.15\varepsilon_F$, (c) $h_{Zf} = 1.1\varepsilon_F$, and (d) $h_{Zf} = 0.95\varepsilon_F$.

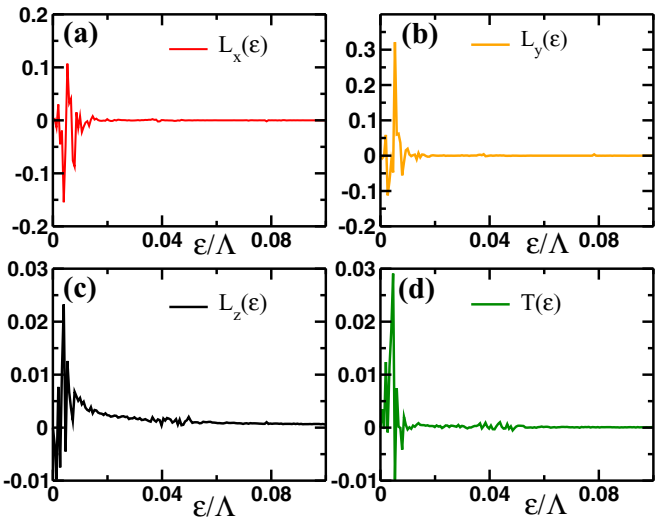

FIG. 9. (Color online) Energy dependence of $\vec{L}(\varepsilon)$ and $T(\varepsilon)$ at time $t\delta = 2.05$ (δ is a level spacing). The values of the remaining parameters are $h_{Zi} = 1.85\varepsilon_F$, $h_{Zf} = 0.5\varepsilon_F$, $n_c = 0.125$, $\Lambda = 10\varepsilon_F$, and $\varepsilon_F = 0.785$.

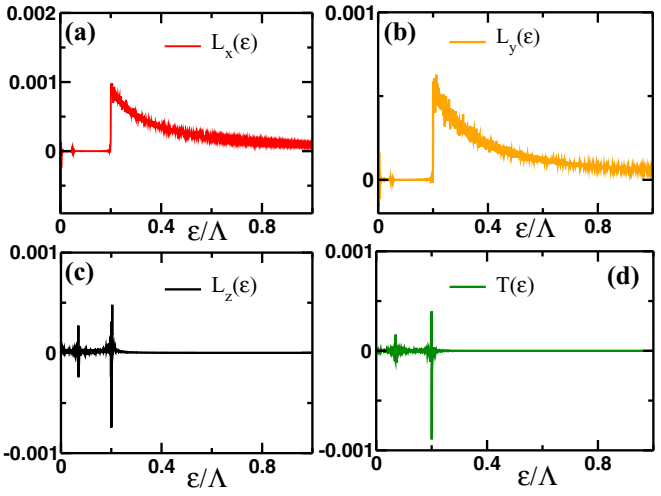

FIG. 10. (Color online) Same as Fig. 9 with $h_{Zf} = 1.25\varepsilon_F$. In contrast to Fig. 9, we see that all components of $\vec{L}(\varepsilon, t \to \infty)$ and $T(\varepsilon, t \to \infty)$ are vanishingly small for all single-particle energies.

equations of motion for the functions $\vec{S}_{\mathbf{k}\lambda}(t)$ decouple from the remaining four equations of motion (2.9) and (2.10). Finally, we make one more observation: This dynamical decoupling happens exactly when the system goes through the Floquet topological transition [33,34] corresponding to the transition from the topologically trivial Floquet spectrum to a steady state with the topologically nontrivial Floquet spectrum. However, the detailed analysis of this transition goes beyond the scope of this paper and we leave it for the future.

V. CONCLUSION

In this paper we have analyzed the far-from-equilibrium pairing dynamics of the spin-orbit coupled fermions in two dimensions with a population imbalance. Specifically, we have considered two separate cases. In the first case the dynamics is initiated by a sudden change of the pairing strength. We found that the steady state with a periodically varying pairing amplitude is realized in much narrower regions of the steady-state phase diagram compared to what happens when the spin-orbit coupling is zero.

Exact integrability of the problem with zero imbalance implies that we can also provide an analytical description for the dynamics initiated by a sudden change of imbalance to zero. We found that when the initial value of the imbalance field h_Z exceeds some critical value h_{c2}, the steady state with a periodically oscillating pairing amplitude is realized and we can determine an analytical expression for $\Delta(t)$.

Perhaps our most interesting result is our finding of the dynamical decoupling for the quenches to finite values of the population imbalance. Specifically, our numerical analysis of the equations of motion showed that when the final value of the population imbalance exceeds some value h_t, the pairing amplitude is determined by a reduced number of pseudospin variables. Interestingly, the value of h_t is a critical value separating the regions of topologically trivial and topologically nontrivial Floquet spectra [34]. Whether topology plays a defining role in the above-mentioned reduction or is just a mere coincidence is an exciting issue, which we leave for the future studies.

ACKNOWLEDGMENTS

M.D. thanks Instituto Superior Tecnico (Lisbon, Portugal), where part of this work was done, for hospitality and acknowledges Fundãcao para a Ciência e a Tecnologia, Grant No. PTDC/FIS/111348/2009, for partial financial support. We thank Boris Altshuler, Antonio Garcia-Garcia, Pedro Ribeiro, Pedro Sacramento, and especially Matthew Foster for illuminating discussions. We would also like to thank Mubarak AlQahtani for the collaboration during the initial stages of this project. This work was financially supported in part by the David and Lucile Packard Foundation (E.A.Y.), NSF Grant No. DMR-1506547 (A.A.K. and M.D.), and MPI-PKS (M.D.).

APPENDIX A: EQUATIONS OF MOTION FOR THE SINGLE-PARTICLE CORRELATORS

In this Appendix we analyze the ground-state properties of the Hamiltonian (2.3) using the equations of motion of the single-particle correlators. The main idea is to derive the set of self-consistent equations describing the collisionless evolution of the pairing amplitude.

Consider the equations of motion for the fermionic operators. We have

$$\begin{aligned} i\frac{\partial}{\partial t}\hat{a}_{\mathbf{k}\lambda}(t) &= \varepsilon_{\mathbf{k}\lambda}\hat{a}_{\mathbf{k}\lambda} - \eta^*_{\mathbf{k}}\Delta[\lambda\Theta_k\hat{a}^\dagger_{-\mathbf{p}\lambda} + \widetilde{\Theta}_k\hat{a}^\dagger_{-\mathbf{p}\bar{\lambda}}], \\ i\frac{\partial}{\partial t}\hat{a}^\dagger_{\mathbf{k}\lambda}(t) &= -\varepsilon_{\mathbf{p}\lambda}\hat{a}^\dagger_{\mathbf{k}\lambda} + \eta_{\mathbf{k}}\overline{\Delta}[\lambda\Theta_k\hat{a}_{-\mathbf{k}\lambda} + \widetilde{\Theta}_k\hat{a}_{-\mathbf{k}\bar{\lambda}}]. \end{aligned} \tag{A1}$$

Next we introduce the following correlation functions, which are diagonal in the new basis:

$$\begin{aligned} G_{\mathbf{p}\lambda}(t_1,t_2) &= -i\langle\hat{T}(\hat{a}_{\mathbf{p}\lambda}(t_1)\hat{a}^\dagger_{\mathbf{p}\lambda}(t_2))\rangle, \\ F_{\mathbf{p}\lambda}(t_1,t_2) &= -i\lambda\eta_{\mathbf{p}}\langle\hat{T}(\hat{a}_{\mathbf{p}\lambda}(t_1)\hat{a}_{-\mathbf{p}\lambda}(t_2))\rangle, \\ \widetilde{G}_{\mathbf{p}\lambda}(t_1,t_2) &= -i\langle\hat{T}(\hat{a}^\dagger_{-\mathbf{p}\lambda}(t_1)\hat{a}_{-\mathbf{p}\lambda}(t_2))\rangle, \\ \overline{F}_{\mathbf{p}\lambda}(t_1,t_2) &= -i\lambda\eta^*_{\mathbf{p}}\langle\hat{T}(\hat{a}^\dagger_{-\mathbf{p}\lambda}(t_1)\hat{a}^\dagger_{\mathbf{p}\lambda}(t_2))\rangle. \end{aligned} \tag{A2}$$

Similarly, we introduce the off-diagonal correlators that account for the scattering of fermions between the two chiral bands:

$$\begin{aligned} \Gamma_{\mathbf{p}\lambda}(t_1,t_2) &= -i\lambda\langle\hat{T}[\hat{a}_{\mathbf{p}\bar{\lambda}}(t_1)\hat{a}^\dagger_{\mathbf{p}\lambda}(t_2)]\rangle, \\ \Phi_{\mathbf{p}\bar{\lambda}}(t_1,t_2) &= -i\eta_{\mathbf{p}}\langle\hat{T}[\hat{a}_{\mathbf{p}\lambda}(t_1)\hat{a}_{-\mathbf{p}\bar{\lambda}}(t_2)]\rangle, \\ \widetilde{\Gamma}_{\mathbf{p}\lambda}(t_1,t_2) &= -i\lambda\langle\hat{T}[\hat{a}^\dagger_{-\mathbf{p}\bar{\lambda}}(t_1)\hat{a}_{-\mathbf{p}\lambda}(t_2)]\rangle, \\ \overline{\Phi}_{\mathbf{p}\lambda}(t_1,t_2) &= -i\eta^*_{\mathbf{p}}\langle\hat{T}[\hat{a}^\dagger_{-\mathbf{p}\bar{\lambda}}(t_1)\hat{a}^\dagger_{\mathbf{p}\lambda}(t_2)]\rangle. \end{aligned} \tag{A3}$$

As a next step one can derive the equations of motion for these correlation functions using (A1).

1. Equations of motion for the diagonal chiral correlators

For the diagonal in the λ correlation functions above we have

$$\left(i\frac{\partial}{\partial t_1} - \varepsilon_{\mathbf{k}\lambda}\right)G_{\mathbf{k}\lambda}(t_1,t_2) + \Delta[\Theta_k\overline{F}_{\mathbf{k}\lambda}(t_1,t_2) + \widetilde{\Theta}_k\overline{\Phi}_{\mathbf{k}\lambda}(t_1,t_2)] = \delta(t_1 - t_2),$$

$$\left(i\frac{\partial}{\partial t_1}-\varepsilon_{\mathbf{k}\bar{\lambda}}\right)\Gamma_{\mathbf{k}\lambda}(t_1,t_2)-\Delta[\Theta_k\overline{\Phi}_{\mathbf{k}\lambda}(t_1,t_2)-\widetilde{\Theta}_k\overline{F}_{\mathbf{k}\lambda}(t_1,t_2)]=0. \tag{A4}$$

Similarly, the equations of motion for the anomalous correlation functions (A3) are

$$\begin{aligned}
&\left(i\frac{\partial}{\partial t_1}+\varepsilon_{\mathbf{k}\lambda}\right)\overline{F}_{\mathbf{k}\lambda}(t_1,t_2)\\
&\quad+\overline{\Delta}[\Theta_k G_{\mathbf{k}\lambda}(t_1,t_2)+\widetilde{\Theta}_k\Gamma_{\mathbf{k}\lambda}(t_1,t_2)]=0,\\
&\left(i\frac{\partial}{\partial t_1}+\varepsilon_{\mathbf{k}\bar{\lambda}}\right)\overline{\Phi}_{\mathbf{k}\lambda}(t_1,t_2)\\
&\quad-\overline{\Delta}[\Theta_k\Gamma_{\mathbf{k}\lambda}(t_1,t_2)-\widetilde{\Theta}_k G_{\mathbf{k}\lambda}(t_1,t_2)]=0,\\
&\left(i\frac{\partial}{\partial t_1}+\varepsilon_{\mathbf{k}\bar{\lambda}}\right)\widetilde{\Gamma}_{\mathbf{k}\lambda}(t_1,t_2)\\
&\quad-\overline{\Delta}[\Theta_k\Phi_{\mathbf{k}\lambda}(t_1,t_2)-\widetilde{\Theta}_k F_{\mathbf{k}\lambda}(t_1,t_2)]=0.
\end{aligned} \tag{A5}$$

In equilibrium, all these correlation functions depend on t_1-t_2 only, so we can perform the Fourier transform and compute them explicitly. It follows that

$$\begin{aligned}
\Gamma_{\mathbf{k}\lambda}(\omega)&=\frac{(\omega+\varepsilon_{\mathbf{k}\bar{\lambda}})\Delta\widetilde{\Theta}_k\overline{F}_{\mathbf{k}\lambda}(\omega)-\Delta^2\Theta_k\widetilde{\Theta}_k G_{\mathbf{k}\lambda}(\omega)}{\omega^2-\varepsilon_{\mathbf{k}\bar{\lambda}}^2-\Delta^2\Theta_k^2},\\
\overline{\Phi}_{\mathbf{k}\lambda}(\omega)&=-\frac{(\omega-\varepsilon_{\mathbf{k}\bar{\lambda}})\overline{\Delta}\widetilde{\Theta}_k G_{\mathbf{k}\lambda}(\omega)+\Delta^2\Theta_k\widetilde{\Theta}_k\overline{F}_{\mathbf{k}\lambda}(\omega)}{\omega^2-\varepsilon_{\mathbf{k}\bar{\lambda}}^2-\Delta^2\Theta_k^2},
\end{aligned} \tag{A6}$$

where we assume that $\Delta=\overline{\Delta}$, i.e., in the ground state the pairing amplitude is real. We have

$$\begin{aligned}
G_{\mathbf{k}\lambda}(\omega)&=-\frac{(\omega+\varepsilon_{\mathbf{k}\lambda})\left[\Theta_k^2\Delta^2+\varepsilon_{\mathbf{k}\bar{\lambda}}^2-\omega^2\right]}{\left(\omega^2-E_{\mathbf{k}\lambda}^2\right)\left(\omega^2-E_{\mathbf{k}\bar{\lambda}}^2\right)}\\
&\quad+\frac{\widetilde{\Theta}_k^2\Delta^2(\omega+\varepsilon_{\mathbf{k}\bar{\lambda}})}{\left(\omega^2-E_{\mathbf{k}\lambda}^2\right)\left(\omega^2-E_{\mathbf{k}\bar{\lambda}}^2\right)},\\
\overline{F}_{\mathbf{k}\lambda}(\omega)&=\frac{\Theta_k\Delta\left[\Delta^2+\varepsilon_{\mathbf{k}\bar{\lambda}}^2-\omega^2\right]}{\left(\omega^2-E_{\mathbf{k}\lambda}^2\right)\left(\omega^2-E_{\mathbf{k}\bar{\lambda}}^2\right)},\\
\Gamma_{\mathbf{k}\lambda}(\omega)&=\frac{2\lambda\Theta_k\widetilde{\Theta}_k\Delta^2R_k}{\left(\omega^2-E_{\mathbf{k}\lambda}^2\right)\left(\omega^2-E_{\mathbf{k}\bar{\lambda}}^2\right)},\\
\overline{\Phi}_{\mathbf{k}\lambda}(\omega)&=\frac{\widetilde{\Theta}_k\Delta[\Delta^2+(\varepsilon_{\mathbf{k}\bar{\lambda}}-\omega)(\omega+\varepsilon_{\mathbf{k}\lambda})]}{\left(\omega^2-E_{\mathbf{k}\lambda}^2\right)\left(\omega^2-E_{\mathbf{k}\bar{\lambda}}^2\right)},\\
\widetilde{\Gamma}_{\mathbf{k}\lambda}(\omega)&=-\frac{2\lambda\Theta_k\widetilde{\Theta}_k\Delta^2R_k}{\left(\omega^2-E_{\mathbf{k}\lambda}^2\right)\left(\omega^2-E_{\mathbf{k}\bar{\lambda}}^2\right)}.
\end{aligned} \tag{A7}$$

This last expression follows from the symmetry properties of the corresponding equations of motion. Note that from these expressions it follows that

$$\begin{aligned}
\overline{\Phi}_{\mathbf{k}\lambda}(\omega)&=\overline{\Phi}_{\mathbf{k}\bar{\lambda}}(-\omega),\\
\Gamma_{\mathbf{k}\lambda}(\omega)&=-\Gamma_{\mathbf{k}\bar{\lambda}}(\omega),\\
\widetilde{\Gamma}_{\mathbf{k}\lambda}(\omega)&=\Gamma_{\mathbf{k}\bar{\lambda}}(\omega).
\end{aligned} \tag{A8}$$

To compute the averages that enter into the self-consistency equation that determines Δ, we employ the Matsubara frequency representation $\omega\to i\omega_n$. Then we perform the summations over the Matsubara frequencies and take the limit $T\to 0$. The resulting functions of momentum are Eqs. (2.11) and (2.12). Note that $L^z\propto\langle a_{\mathbf{k}\bar{\lambda}}^\dagger a_{\mathbf{k}\lambda}\rangle$ is generated already within the mean-field theory despite the fact that the terms proportional to $a_{\mathbf{k}\bar{\lambda}}^\dagger a_{\mathbf{k}\lambda}$ do not enter into the Hamiltonian. In what follows we also consider the function

$$T_{\mathbf{k}}^z=\frac{1}{2}T\sum_{i\omega_n}[\Gamma_{\mathbf{k}\bar{\lambda}}(i\omega_n)+\Gamma_{\mathbf{k}\lambda}(i\omega_n)], \tag{A9}$$

which is zero in the ground state; however, it is generated during the evolution.

Our goal now is to derive the equations of motion for all the correlation functions above as a function of

$$t=\frac{t_1+t_2}{2}. \tag{A10}$$

Since both normal and anomalous correlators (A2) and (A3) depend on $\tau=t_1-t_2$, the order parameter $\Delta(t)$ is a function of total time t only. Thus, in what follows we consider $\tau=0$.

From the equations of motion for the fermionic operators (A1) and Eqs. (A2) and (A3) it follows that

$$\begin{aligned}
&i\frac{d}{dt}G_{\mathbf{k}\lambda}(t)+\Delta(t)[\Theta_k\overline{F}_{\mathbf{k}\lambda}(t)+\widetilde{\Theta}_k\overline{\Phi}_{\mathbf{k}\lambda}(t)]\\
&\quad-\overline{\Delta}(t)[\Theta_k F_{\mathbf{k}\lambda}(t)+\widetilde{\Theta}_k\Phi_{\mathbf{k}\bar{\lambda}}(t)]=0,\\
&\left(i\frac{d}{dt}-2\varepsilon_{\mathbf{k}\lambda}\right)F_{\mathbf{k}\lambda}(t)+\Delta(t)\{\Theta_k[\widetilde{G}_{\mathbf{k}\lambda}(t)-G_{\mathbf{k}\lambda}(t)]\\
&\quad+\widetilde{\Theta}_k[\widetilde{\Gamma}_{\mathbf{k}\lambda}(t)-\Gamma_{\mathbf{k}\lambda}(t)]\}=0.
\end{aligned} \tag{A11}$$

Similarly, for the remaining two correlation functions that are diagonal in new basis we find

$$\begin{aligned}
&i\frac{d}{dt}\widetilde{G}_{\mathbf{k}\lambda}(t)+\overline{\Delta}(t)[\Theta_k F_{\mathbf{k}\lambda}(t)+\widetilde{\Theta}_k\Phi_{\mathbf{k}\bar{\lambda}}(t)]\\
&\quad-\Delta(t)[\Theta_k\overline{F}_{\mathbf{k}\lambda}(t)+\widetilde{\Theta}_k\overline{\Phi}_{\mathbf{k}\lambda}(t)]=0,\\
&\left(i\frac{d}{dt}+2\varepsilon_{\mathbf{k}\lambda}\right)\overline{F}_{\mathbf{k}\lambda}(t)+\overline{\Delta}(t)\{\Theta_k[G_{\mathbf{k}\lambda}(t)-\widetilde{G}_{\mathbf{k}\lambda}(t)]\\
&\quad+\widetilde{\Theta}_k[\Gamma_{\mathbf{k}\lambda}(t)-\widetilde{\Gamma}_{\mathbf{k}\lambda}(t)]\}=0.
\end{aligned} \tag{A12}$$

From the equations for the normal propagators it follows that

$$\widetilde{G}_{\mathbf{k}\lambda}(t)=-G_{\mathbf{k}\lambda}(t). \tag{A13}$$

Let us introduce the functions

$$\begin{aligned}
S_{\mathbf{k}\lambda}^z(t)&=\frac{i}{2}[\tilde{G}_{\mathbf{k}\lambda}(t)-G_{\mathbf{k}\lambda}(t)],\\
S_{\mathbf{k}\lambda}^-(t)&=S_{\mathbf{k}\lambda}^x(t)-iS_{\mathbf{k}\lambda}^y(t)=-iF_{\mathbf{k}\lambda}(t),\\
S_{\mathbf{k}\lambda}^+(t)&=S_{\mathbf{k}\lambda}^x(t)+iS_{\mathbf{k}\lambda}^y(t)=-i\overline{F}_{\mathbf{k}\lambda}(t)
\end{aligned} \tag{A14}$$

and

$$\begin{aligned}
L_{\mathbf{k}\lambda}^z(t)&=\frac{i}{2}[\widetilde{\Gamma}_{\mathbf{k}\lambda}(t)-\Gamma_{\mathbf{k}\lambda}(t)],\\
L_{\mathbf{k}\lambda}^-(t)&=L_{\mathbf{k}\lambda}^x(t)-iL_{\mathbf{k}\lambda}^y(t)=-i\Phi_{\mathbf{k}\bar{\lambda}}(t),\\
L_{\mathbf{k}\lambda}^+(t)&=L_{\mathbf{k}\lambda}^x(t)+iL_{\mathbf{k}\lambda}^y(t)=-i\overline{\Phi}_{\mathbf{k}\lambda}(t).
\end{aligned} \tag{A15}$$

In terms of these new functions, the self-consistency equation for the pairing amplitude reads

$$\Delta(t) = g\sum_{\mathbf{k}\mu}[\Theta_k S^-_{\mathbf{k}\mu}(t) + \widetilde{\Theta}_k L^-_{\mathbf{k}\mu}(t)]. \tag{A16}$$

2. Equations of motion for the off-diagonal chiral correlators

The remaining equations of motion for the components of $\vec{L}$ can be derived in the same way. Let us obtain the equations of motion for $\Gamma_{\mathbf{k}\lambda}(t)$. In what follows the only relations we use are

$$\begin{aligned}\Gamma_{\mathbf{k}\bar{\lambda}}(t) &= \widetilde{\Gamma}_{\mathbf{k}\lambda}(t),\\ \overline{\Phi}_{\mathbf{k}\lambda}(t) &= \overline{\Phi}_{\mathbf{k}\bar{\lambda}}(t),\\ \widetilde{G}_{\mathbf{k}\lambda} &= -G_{\mathbf{k}\lambda}.\end{aligned} \tag{A17}$$

The validity of these relations will be proven when we analyze the equilibrium. We need to keep in mind, however, that given the second relation, we expect that the equations of motion for $L^{\pm}_{\mathbf{k}\lambda}(t)$ should not depend on the chiral band index λ. The equations of motion for the correlator $\overline{\Phi}_{\mathbf{k}\lambda}(t_1,t_2)$ are

$$\begin{aligned}&\left(i\frac{\partial}{\partial t_1} + \varepsilon_{\mathbf{k}\bar{\lambda}}\right)\overline{\Phi}_{\mathbf{k}\lambda}(t_1,t_2)\\ &\quad -\overline{\Delta}[\Theta_k\Gamma_{\mathbf{k}\lambda}(t_1,t_2) - \widetilde{\Theta}_k G_{\mathbf{k}\lambda}(t_1,t_2)] = 0,\\ &\left(i\frac{\partial}{\partial t_2} + \varepsilon_{\mathbf{k}\lambda}\right)\overline{\Phi}_{\mathbf{k}\lambda}(t_1,t_2)\\ &\quad -\overline{\Delta}[\Theta_k\widetilde{\Gamma}_{\mathbf{k}\lambda}(t_1,t_2) + \widetilde{\Theta}_k\widetilde{G}_{\mathbf{k}\bar{\lambda}}(t_1,t_2)] = 0,\end{aligned} \tag{A18}$$

where we used $\eta_{-\mathbf{p}} = -\eta_{\mathbf{p}}$. Adding these two equations yields

$$\left(i\frac{\partial}{\partial t} + 2\epsilon_{\mathbf{k}}\right)\overline{\Phi}_{\mathbf{k}\lambda}(t) - \widetilde{\Theta}_k\overline{\Delta}(t)[\widetilde{G}_{\mathbf{k}\bar{\lambda}}(t) - G_{\mathbf{k}\lambda}(t)] = 0. \tag{A19}$$

From this equation we can immediately obtain the equations of motion for $L^{x,y}_{\mathbf{k}\lambda}$ using Eqs. (A14) and (A15).

Finally, we derive the equation of motion for

$$T_{\mathbf{k}}(t) = \frac{\Gamma_{\mathbf{k}\lambda}(t) + \Gamma_{\mathbf{k}\bar{\lambda}}(t)}{2}. \tag{A20}$$

Before writing down this equation, let us first obtain the equations of motion for $\Gamma_{\mathbf{k}\lambda}$ and $\widetilde{\Gamma}_{\mathbf{k}\lambda}$. We have

$$\begin{aligned}&\left(i\frac{\partial}{\partial t_1} - \varepsilon_{\mathbf{k}\bar{\lambda}}\right)\Gamma_{\mathbf{k}\lambda}(t_1,t_2)\\ &\quad -\Delta[\Theta_k\overline{\Phi}_{\mathbf{k}\lambda}(t_1,t_2) - \widetilde{\Theta}_k\overline{F}_{\mathbf{k}\lambda}(t_1,t_2)] = 0,\\ &\left(i\frac{\partial}{\partial t_2} + \varepsilon_{\mathbf{k}\lambda}\right)\Gamma_{\mathbf{k}\lambda}(t_1,t_2)\\ &\quad -\overline{\Delta}[\Theta_k\Phi_{\mathbf{k}\lambda}(t_1,t_2) - \widetilde{\Theta}_k F_{\mathbf{k}\bar{\lambda}}(t_1,t_2)] = 0,\\ &\left(i\frac{\partial}{\partial t_1} + \varepsilon_{\mathbf{k}\bar{\lambda}}\right)\widetilde{\Gamma}_{\mathbf{k}\lambda}(t_1,t_2)\\ &\quad -\overline{\Delta}[\Theta_k\Phi_{\mathbf{k}\lambda}(t_1,t_2) - \widetilde{\Theta}_k F_{\mathbf{k}\lambda}(t_1,t_2)] = 0,\\ &\left(i\frac{\partial}{\partial t_2} - \varepsilon_{\mathbf{k}\lambda}\right)\widetilde{\Gamma}_{\mathbf{k}\lambda}(t_1,t_2)\\ &\quad -\Delta[\Theta_k\overline{\Phi}_{\mathbf{k}\lambda}(t_1,t_2) - \widetilde{\Theta}_k\overline{F}_{\mathbf{k}\bar{\lambda}}(t_1,t_2)] = 0,\end{aligned} \tag{A21}$$

where we have employed (A17), $\eta_{-\mathbf{p}} = -\eta_{\mathbf{p}}$, and $\lambda\bar{\lambda} = -1$. Adding the first and second equations and then the third and fourth ones and setting $\tau = t_1 - t_2 = 0$ yields

$$\begin{aligned}&\left(i\frac{\partial}{\partial t} - 2\lambda R_k\right)\Gamma_{\mathbf{k}\lambda}(t) - \Theta_k[\Delta\overline{\Phi}_{\mathbf{k}\lambda}(t) + \overline{\Delta}\Phi_{\mathbf{k}\lambda}(t)]\\ &\quad + \widetilde{\Theta}_k[\Delta\overline{F}_{\mathbf{k}\lambda}(t) + \overline{\Delta}F_{\mathbf{k}\bar{\lambda}}(t)] = 0,\\ &\left(i\frac{\partial}{\partial t} + 2\lambda R_k\right)\widetilde{\Gamma}_{\mathbf{k}\lambda}(t) - \Theta_k[\Delta\overline{\Phi}_{\mathbf{k}\lambda}(t) + \overline{\Delta}\Phi_{\mathbf{k}\lambda}(t)]\\ &\quad + \widetilde{\Theta}_k[\overline{\Delta}F_{\mathbf{k}\lambda}(t) + \Delta\overline{F}_{\mathbf{k}\bar{\lambda}}(t)] = 0,\end{aligned} \tag{A22}$$

where $R_k = \sqrt{V_z^2 + \alpha_{\mathrm{SO}}^2 k^2}$. From these equations we see that, given the property (A17), we have

$$\Gamma_{\mathbf{k}\lambda} = Z_{\mathbf{k}} + iL^z_{\mathbf{k}\lambda}. \tag{A23}$$

It is now straightforward to verify that the equations of motion for these objects are the same as Eqs. (2.7), (2.9), and (2.10). Thus we have ten equations of motion. These equations are decoupled into six plus four when either $\alpha_{\mathrm{SO}} = 0$ or $h_Z = 0$. Note that neither L_z nor $T_{\mathbf{k}}$ enters into the Hamiltonian and both are generated in the course of the dynamics.

APPENDIX B: GENERAL RELATIONS BETWEEN THE COMPONENTS' AUXILIARY FUNCTIONS IN EQUILIBRIUM

We assume that in equilibrium $\Delta_x = \Delta$ and $\Delta_y = 0$. This implies that at $t = 0$ both $S^y_{\mathbf{k}\lambda} = 0$ and $L^y_{\mathbf{k}\lambda} = 0$, in accordance with the self-consistency conditions. This guarantees that seven out of ten equations (2.7), (2.9), and (2.10) for the components of vectors $\vec{S}$, $\vec{L}$, and $T_{\mathbf{k}}$ are identically zero. The remaining three equations are

$$\begin{aligned}\varepsilon_{\mathbf{k}\lambda}S^x_{\mathbf{k}\lambda} + \Delta\cdot\left(\Theta_k S^z_{\mathbf{k}\lambda} + \widetilde{\Theta}_k L^z_{\mathbf{k}\lambda}\right) &= 0,\\ 2\epsilon_{\mathbf{k}}L^x_{\mathbf{k}\lambda} + \widetilde{\Theta}_k\Delta\left[S^z_{\mathbf{k}\lambda} + S^z_{\mathbf{k}\bar{\lambda}}\right] &= 0,\\ 2\lambda R_k L^z_{\mathbf{k}\lambda} + \Delta\left\{2\Theta_k L^x_{\mathbf{k}\lambda} - \widetilde{\Theta}_k\left[S^x_{\mathbf{k}\lambda} + S^x_{\mathbf{k}\bar{\lambda}}\right]\right\} &= 0.\end{aligned} \tag{B1}$$

Let us verify if the expressions for the spin components satisfy (B1). For the first two equations we find

$$\begin{aligned}\Delta\left[\Theta_k S^z_{\mathbf{k}\lambda} + \widetilde{\Theta}_k L^z_{\mathbf{k}\lambda}\right] &= -\varepsilon_{\mathbf{k}\lambda}S^x_{\mathbf{k}\lambda},\\ \widetilde{\Theta}_k\Delta\left[S^z_{\mathbf{k}\lambda} + S^z_{\mathbf{k}\bar{\lambda}}\right] &= -2\epsilon_{\mathbf{k}}L^x_{\mathbf{k}\lambda}.\end{aligned} \tag{B2}$$

Finally, let us check the third of Eqs. (B1):

$$2\Theta_k\Delta L^x_{\mathbf{k}\lambda} - \widetilde{\Theta}_k\Delta\left[S^x_{\mathbf{k}\lambda} + S^x_{\mathbf{k}\bar{\lambda}}\right] = -\frac{4\Theta_k\widetilde{\Theta}_k\Delta^2R_k^2}{2E_{\mathbf{k}\lambda}E_{\mathbf{k}\bar{\lambda}}(E_{\mathbf{k}\lambda} + E_{\mathbf{k}\bar{\lambda}})}. \tag{B3}$$

In contrast,

$$\begin{aligned}2\lambda R_k L^z_{\mathbf{k}\lambda} &= 2\lambda R_k\frac{\Theta_k\widetilde{\Theta}_k\Delta^2(\varepsilon_{\mathbf{k}\bar{\lambda}} - \varepsilon_{\mathbf{k}\lambda})}{2E_{\mathbf{k}\lambda}E_{\mathbf{k}\bar{\lambda}}(E_{\mathbf{k}\lambda} + E_{\mathbf{k}\bar{\lambda}})}\\ &= \frac{4\Theta_k\widetilde{\Theta}_k\Delta^2R_k^2}{2E_{\mathbf{k}\lambda}E_{\mathbf{k}\bar{\lambda}}(E_{\mathbf{k}\lambda} + E_{\mathbf{k}\bar{\lambda}})}.\end{aligned} \tag{B4}$$

Thus the third of Eqs. (B1) holds.

[1] L. P. Gor'kov and E. I. Rashba, Phys. Rev. Lett. **87**, 037004 (2001).
[2] Y. J. Lin, K. Jimenez-Garcia, and I. B. Spielman, Nature (London) **471**, 83 (2011).
[3] L. He and X.-G. Huang, Phys. Rev. Lett. **108**, 145302 (2012).
[4] L. He and X.-G. Huang, Phys. Rev. A **86**, 043618 (2012).
[5] L. He and X.-G. Huang, Ann. Phys. (NY) **337**, 163 (2013).
[6] M. Chapman and C. S. de Melo, Nature (London) **471**, 41 (2011).
[7] J.-Y. Zhang, S.-C. Ji, Z. Chen, L. Zhang, Z.-D. Du, B. Yan, G.-S. Pan, B. Zhao, Y.-J. Deng, H. Zhai, *et al.*, Phys. Rev. Lett. **109**, 115301 (2012).
[8] P. Wang, Z.-Q. Yu, Z. Fu, J. Miao, L. Huang, S. Chai, H. Zhai, and J. Zhang, Phys. Rev. Lett. **109**, 095301 (2012).
[9] L. W. Cheuk, A. T. Sommer, Z. Hadzibabic, T. Yefsah, W. S. Bakr, and M. W. Zwierlein, Phys. Rev. Lett. **109**, 095302 (2012).
[10] C. Qu, C. Hamner, M. Gong, C. Zhang, and P. Engels, Phys. Rev. A **88**, 021604 (2013).
[11] C. L. Kane and E. J. Mele, Phys. Rev. Lett. **95**, 146802 (2005).
[12] L. Fu, C. L. Kane, and E. J. Mele, Phys. Rev. Lett. **98**, 106803 (2007).
[13] L. Fu and C. L. Kane, Phys. Rev. B **76**, 045302 (2007).
[14] B. A. Bernevig, T. L. Hughes, and S.-C. Zhang, Science **314**, 1757 (2006).
[15] M. Sato, Y. Takahashi, and S. Fujimoto, Phys. Rev. Lett. **103**, 020401 (2009).
[16] M. Sato, Y. Takahashi, and S. Fujimoto, Phys. Rev. B **82**, 134521 (2010).
[17] M. Z. Hasan and C. L. Kane, Rev. Mod. Phys. **82**, 3045 (2010).
[18] X.-L. Qi and S.-C. Zhang, Rev. Mod. Phys. **83**, 1057 (2011).
[19] A. Ohtomo and H. Y. Hwang, Nature (London) **427**, 423 (2004).
[20] N. Reyren, S. Thiel, A. D. Caviglia, L. F. Kourkoutis, G. Hammerl, C. Richter, C. W. Schneider, T. Kopp, A.-S. Retschi, D. Jaccard, *et al.*, Science **317**, 1196 (2007).
[21] A. D. Caviglia, S. Gariglio, N. Reyren, D. Jaccard, T. Schneider, M. Gabay, S. Thiel, G. Hammerl, J. Mannhart, and J. M. Triscone, Nature (London) **456**, 624 (2008).
[22] M. S. Scheurer and J. Schmalian, Nat. Commun. **6**, 6005 (2015).
[23] J.-i. Inoue and A. Tanaka, Phys. Rev. Lett. **105**, 017401 (2010).
[24] T. Kitagawa, E. Berg, M. Rudner, and E. Demler, Phys. Rev. B **82**, 235114 (2010).
[25] N. H. Lindner, G. Refael, and V. Galitski, Nat. Phys. **7**, 490 (2011).
[26] L. Jiang, T. Kitagawa, J. Alicea, A. R. Akhmerov, D. Pekker, G. Refael, J. I. Cirac, E. Demler, M. D. Lukin, and P. Zoller, Phys. Rev. Lett. **106**, 220402 (2011).
[27] Q.-J. Tong, J.-H. An, J. Gong, H.-G. Luo, and C. H. Oh, Phys. Rev. B **87**, 201109 (2013).
[28] D. E. Liu, A. Levchenko, and H. U. Baranger, Phys. Rev. Lett. **111**, 047002 (2013).
[29] X. Yang, arXiv:1410.5035.
[30] A. Poudel, G. Ortiz, and L. Viola, Europhys. Lett. **110**, 17004 (2015).
[31] P. D. Sacramento, Phys. Rev. B **91**, 214518 (2015).
[32] M. S. Foster, M. Dzero, V. Gurarie, and E. A. Yuzbashyan, Phys. Rev. B **88**, 104511 (2013).
[33] M. S. Foster, V. Gurarie, M. Dzero, and E. A. Yuzbashyan, Phys. Rev. Lett. **113**, 076403 (2014).
[34] Y. Dong, L. Dong, M. Gong, and H. Pu, Nat. Commun. **6**, 6103 (2015).
[35] R. A. Barankov, L. S. Levitov, and B. Z. Spivak, Phys. Rev. Lett. **93**, 160401 (2004).
[36] E. A. Yuzbashyan and M. Dzero, Phys. Rev. Lett. **96**, 230404 (2006).
[37] E. A. Yuzbashyan, O. Tsyplyatyev, and B. L. Altshuler, Phys. Rev. Lett. **96**, 097005 (2006).
[38] R. A. Barankov and L. S. Levitov, Phys. Rev. A **73**, 033614 (2006).
[39] R. A. Barankov and L. S. Levitov, arXiv:0704.1292.
[40] E. A. Yuzbashyan, M. Dzero, V. Gurarie, and M. S. Foster, Phys. Rev. A **91**, 033628 (2015).
[41] E. A. Yuzbashyan, Phys. Rev. B **78**, 184507 (2008).
[42] V. S. Shumeiko, Dynamics of electronic system with off-diagonal order parameter and non-linear resonant phenomena in superconductors, Ph.D. thesis, Institute for Low Temperature Physics and Engineering, 1990.
[43] J. Bardeen, L. N. Cooper, and J. R. Schrieffer, Phys. Rev. **108**, 1175 (1957).
[44] P. W. Anderson, Phys. Rev. **112**, 1900 (1958).
[45] E. A. Yuzbashyan, B. L. Altshuler, V. B. Kuznetsov, and V. Z. Enolskii, J. Phys. A **38**, 7831 (2005).
[46] E. A. Yuzbashyan, B. L. Altshuler, V. B. Kuznetsov, and V. Z. Enolskii, Phys. Rev. B **72**, 220503 (2005).
[47] A. Nahum and E. Bettelheim, Phys. Rev. B **78**, 184510 (2008).
[48] A. M. Clogston, Phys. Rev. Lett. **9**, 266 (1962).
[49] B. S. Chandrasekhar, Appl. Phys. Lett. **1**, 7 (1962).